



# Vir1p, the yeast homolog of virilizer, is required for mRNA m<sup>6</sup>A methylation and meiosis

Zachory M. Park ,<sup>1</sup> Ethan Belnap,<sup>1</sup> Matthew Remillard,<sup>2</sup> Mark D. Rose <sup>1,2,\*</sup><sup>1</sup>Department of Biology, Georgetown University, Washington, DC 20057, USA<sup>2</sup>Department of Molecular Biology, Princeton University, Princeton, NJ 08544, USA

\*Corresponding author: Email: mark.rose@georgetown.edu

## Abstract

N<sup>6</sup>-Methyladenosine (m<sup>6</sup>A) is among the most abundant modifications of eukaryotic mRNAs. mRNA methylation regulates many biological processes including playing an essential role in meiosis. During meiosis in the budding yeast, *Saccharomyces cerevisiae*, m<sup>6</sup>A levels peak early, before the initiation of the meiotic divisions. High-throughput studies suggested, and this work confirms that the uncharacterized protein Ygl036wp interacts with Kar4p, a component of the mRNA m<sup>6</sup>A-methyltransferase complex. Protein structure programs predict that Ygl036wp folds like VIRMA/Virilizer/VIR, which is involved in mRNA m<sup>6</sup>A-methylation in higher eukaryotes. In addition, Ygl036wp contains conserved motifs shared with VIRMA/Virilizer/VIR. Accordingly, we propose the name *VIR1* for budding yeast ortholog of *VIRMA/Virilizer/VIR 1*. Vir1p interacts with all other members of the yeast methyltransferase complex and is itself required for mRNA m<sup>6</sup>A methylation and meiosis. In the absence of Vir1p proteins comprising the methyltransferase complex become unstable, suggesting that Vir1p acts as a scaffold for the complex. The *vir1Δ/Δ* mutant is defective for the premeiotic S-phase, which is suppressed by overexpression of the early meiotic transcription factor *IME1*; additional overexpression of the translational regulator *RIM4* is required for sporulation. The *vir1Δ/Δ* mutant exhibits reduced levels of *IME1* mRNA, as well as transcripts within *Ime1p*'s regulon. Suppression by *IME1* revealed an additional defect in the expression of the middle meiotic transcription factor, *Ndt80p* (and genes in its regulon), which is rescued by overexpression of *RIM4*. Together, these data suggest that Vir1p is required for cells to initiate the meiotic program and for progression through the meiotic divisions and spore formation.

**Keywords:** meiosis, methylation, posttranscriptional regulation, sporulation, methyltransferase

## Introduction

mRNA m<sup>6</sup>A methylation is a ubiquitous eukaryotic mRNA modification implicated in a host of important biological processes including gametogenesis (Lasman et al. 2020). Mis-regulation of m<sup>6</sup>A methylation is observed in a variety of diseases including cancer (Shen et al. 2020). It is estimated that about 0.1–0.4% of all adenosine nucleotides in mammalian mRNAs are methylated (Yang et al. 2018; Zaccara et al. 2019; Shen et al. 2020). Although m<sup>6</sup>A methylation has been known for several decades (Perry and Kelley 1974), questions remain about the underlying mechanisms targeting m<sup>6</sup>A to specific regions of mRNAs as well as m<sup>6</sup>A's impact on the downstream fate of the modified mRNAs.

In mammals, mRNA methylation is catalyzed by a core complex comprised of METTL3, METTL14, and Wilms' Tumor Associated Protein (WTAP) (Bujnicki et al. 2002; Yang et al. 2018; Zaccara et al. 2019). Accessory proteins include VIRMA/Virilizer/Vir, HAKAI, RBM15/15B, and ZC3H13. METTL3 is the catalytic subunit and forms a heterodimer with a paralogue, METTL14, which facilitates mRNA binding (Bujnicki et al. 2002; Liu et al. 2014; Wang, Doxtader, et al. 2016; Wang, Feng, et al. 2016). WTAP is thought to link the METTL3/14 heterodimer to accessory proteins (Horiuchi et al. 2013). VIRMA stabilizes the complex and plays a role in the site selection of the modification (Yue et al. 2018). HAKAI is an E3 ubiquitin ligase and its role in the complex is not well

understood (Ruzicka et al. 2017). RBM15/15B are paralogous RNA-binding proteins that may also be involved in site selection (Lence et al. 2016; Patil et al. 2016). ZC3H13 links RBM15/15B to WTAP and is responsible for anchoring the complex in the nucleus (Guo et al. 2018; Knuckles et al. 2018; Wen et al. 2018). These proteins make up the "writer" complex, which is responsible for the methylation and the specificity of the modification. Interestingly, METTL3 also engages in a noncatalytic function involving interactions with poly-A binding protein (PABP) and translation initiation factors to enhance the translation of mRNAs in an m<sup>6</sup>A-independent manner (Lin et al. 2016; Wei et al. 2022).

The budding yeast (*Saccharomyces cerevisiae*) contains an mRNA m<sup>6</sup>A methylation complex that is conserved with higher eukaryotes. The yeast complex comprises Ime4p (homolog of METTL3), Kar4p (homolog of METTL14), Mum2p (homolog of WTAP), and Slz1p (homolog of ZC3H13) (Agarwala et al. 2012; Ensinnck et al. 2023; Park, Sporer, et al. 2023). Recent work identified the cytoplasmic dynein light chain, Dyn2p, as also being involved in mRNA methylation (Ensinnck et al. 2023). Unlike in higher eukaryotes, mRNA methylation is not found in mitotic mRNA. However, like other eukaryotes, mRNA methylation regulates meiosis in yeast (Clancy et al. 2002; Agarwala et al. 2012; Schwartz et al. 2013).

The meiotic program in yeast is initiated by starvation for nitrogen and a fermentable carbon source, leading to the expression of the early meiotic transcription factor, *IME1*. *Ime1p* activates the

expression of early genes required for premeiotic DNA synthesis and the subsequent initiation of meiotic recombination (Kassir et al. 1988; Smith and Mitchell 1989; Smith et al. 1990; Smith et al. 1993; Mandel et al. 1994; Kassir et al. 2003; Neiman 2011). *Ime1p* also induces the expression of *Ime2p*, a kinase that facilitates premeiotic DNA synthesis and activates the full expression of the middle meiotic transcription factor, *Ndt80p* (Mitchell et al. 1990; Yoshida et al. 1990; Kominami et al. 1993; Smith et al. 1993; Foiani et al. 1996; Dirick et al. 1998; Guttmann-Raviv et al. 2001; Benjamin et al. 2003; Purnapatre et al. 2005; Schindler and Winter 2006; Sedgwick et al. 2006; Sawarynski et al. 2007; Brush et al. 2012). *Ndt80p* regulates the expression of genes required for the completion of meiotic recombination, progression through the meiotic divisions, and spore maturation (Chu et al. 1998; Chu and Herskowitz 1998; Pak and Segall 2002; Kassir et al. 2003; Shubassi et al. 2003; Sopko and Stuart 2004; Gurevich and Kassir 2010; Winter 2012). Another key regulator of meiosis is the RNA-binding protein, *Rim4p*. *Rim4p* was first identified as an activator of the initial events of meiosis (Soushko and Mitchell 2000; Deng and Saunders 2001), but its role as a negative regulator of translation during meiosis is better understood (Berchowitz et al. 2013, 2015; Jin et al. 2015). As a negative regulator, *Rim4p* forms amyloid-like aggregates that bind transcripts before their protein products are required (Berchowitz et al. 2015).

In yeast,  $m^6A$  levels peak before the initiation of the meiotic divisions (Agarwala et al. 2012). The  $m^6A$  modification is concentrated near stop codons and is associated with translating ribosomes (Bodi et al. 2010; Schwartz et al. 2013; Bodi et al. 2015). Similar to the impact on mammalian transcripts (Shi et al. 2017),  $m^6A$  modification appears to facilitate both the translation and decay of transcripts important for early meiotic processes, including recombination (Varier et al. 2022; Scutenaire et al. 2023). For example, mRNA methylation impacts the negative transcriptional regulator of *IME1*, *RME1*. Methylation of *RME1* mRNA results in more rapid decay; the subsequent reduction in *Rme1p* levels facilitates the efficient expression of *IME1* and induction of the meiotic program (Bushkin et al. 2019). However, the methyltransferase complex appears to also have a noncatalytic function that is required for licensing the cells to fully complete meiotic recombination and subsequent divisions (Bushkin et al. 2019; Park, Remillard, et al. 2023; Park, Sporer, et al. 2023). Similar to the mammalian complex, the noncatalytic function may regulate the translation of transcripts in an  $m^6A$ -independent manner.

Recent work revealed that the yeast karyogamy protein and homolog of METTL14, *Kar4p*, is required for efficient mRNA methylation and meiosis (Ensinck et al. 2023; Park, Sporer, et al. 2023). A screen for separation of function alleles of *Kar4p* identified three distinct functions, one in mating (Kurihara et al. 1996; Lahav et al. 2007) and two in meiosis termed *Mei* and *Spo* (Park, Sporer, et al. 2023). Loss of *Kar4p* is partially suppressed by overexpression of *IME1* and fully suppressed by co-overexpression of *IME1* and *RIM4*. *IME1* overexpression permits premeiotic DNA synthesis in *kar4Δ/Δ* (*Mei* function), but defects remain in the timing of meiotic recombination, expression of *NDT80*, and the levels of proteins required for spore formation (*Spo* function). *IME1* and *RIM4* co-overexpression also permits sporulation in *mum2Δ/Δ* and *ime4Δ/Δ* mutants. Overexpression of *IME1* alone rescues the meiotic defect of a catalytically dead mutant of *Ime4p* (Park, Sporer, et al. 2023) suggesting that the “*Mei*” function is associated with  $m^6A$  methylation. The defects remaining in the deletion mutants after *IME1* overexpression, which require *Rim4p* overexpression to be suppressed, are presumed to be associated with the noncatalytic function of the complex. Finally, given *Slz1p*'s role

in anchoring the complex in the nucleus, suppression of *slz1Δ/Δ* by *IME1* overexpression alone suggests that the noncatalytic function occurs in the cytoplasm.

The conservation of the methyltransferase complex led us to hypothesize that there may be other components in yeast yet to be identified. Immunoprecipitation-mass spectrometry (IP-MS) detected a previously uncharacterized protein, *Ygl036wp*, which interacts with *Kar4p* and all other known members of the yeast methyltransferase complex. Moreover, *Ygl036wp* is required for mRNA  $m^6A$  methylation, stability of the complex, and meiosis. *Ygl036wp* is a remote homolog of *VIRMA/Virilizer/VIR*, and we, therefore, have renamed the gene *VIR1* for budding yeast ortholog of *VIRMA/Virilizer/VIR* 1. Given that many of the mammalian methyltransferase components are essential (Yue et al. 2018; Poh et al. 2022), these findings position yeast as an excellent model for furthering our understanding of mRNA  $m^6A$  methylation.

## Materials and methods

### Strains, media, and sporulation conditions

All yeast strains used in this paper are described in Supplementary Table 1. In general, strains are in the S288c background. In some specific experiments, the SK1 strain background was used, as indicated. Plasmids used in the experiments are described in Supplementary Table 2.

Yeast cells from the S288c background were first grown overnight at 30°C in either yeast peptone dextrose (YPD) (yeast extract (1% w/v), peptone (2% w/v), and dextrose 2%) or synthetic media lacking a nutrient to maintain a selection of a plasmid. Overnight cultures were diluted to an optical density (OD) of 0.1 in yeast peptone acetate (YPA) (yeast extract (1% w/v), peptone (2% w/v), and potassium acetate (1% w/v)) and grown for 16–18 hours at 30°C. YPA cultures were then moved into 1% (w/v) potassium acetate (*Spo*) media supplemented with uracil, histidine, and leucine at an OD of 0.5. Cultures were sporulated for various amounts of time at 26°C. For experiments involving overexpression, estradiol was added to cultures immediately after moving them to *Spo* media at a final concentration of 1  $\mu$ M. Experiments using the SK1 strain background ( $m^6A$  measurements and *Ime4p* stability) were handled in much the same way with the only two exceptions being sporulation cultures were diluted to a final OD of 2.0 and were sporulated at 30°C consistent with previously reported sporulation protocols for this strain background (Agarwala et al. 2012).

### IP-MS

For each time point, 200 ml of sporulating culture at an  $OD_{600}$  of 1 were pelleted, washed with water, and flash frozen by liquid nitrogen. Samples were prepared according to the Thermo Scientific Pierce Magnetic HA-Tag IP/Co-IP Kit (88838). Cells were lysed using a FastPrep (MP) bead beater (5  $\times$  90 second runs at 4°C) and acid-washed glass beads (BioSpec), centrifuged, and lysate prepared according to kit protocol.

Eluted immune-precipitated samples were dried in a speedvac to completion and the residual proteins were resuspended in 200  $\mu$ l of 50 mM ammonium bicarbonate pH 8. TCEP (tris(2-carboxyethyl)phosphine) was added to a final concentration of 5 mM and incubated at 60°C for 20 min. 15 mM chloroacetamide was added and incubated in the dark at room temperature for a further 30 min. One microgram of Trypsin Gold (Promega) was added to each sample and incubated in an end-over-end mixer at 37°C for 16 hours. An additional 0.25  $\mu$ g of Trypsin Gold was added and incubated in an end-over-end mixer at 37°C for another

3 hours. Samples were acidified by adding trifluoroacetic acid to a final concentration of 0.2% and were desalted using styrenedivinyl benzene reverse phase sulfonate tips (Rappsilber et al. 2007). Samples were dried completely in a speedvac and resuspended with 20  $\mu$ l of 0.1% formic acid pH 3. Five microliters were injected per run using an Easy-nLC 1000 UPLC system. Samples were loaded directly onto a 45 cm long 75  $\mu$ m inner diameter nano capillary column packed with 1.9  $\mu$ m C18-AQ (Dr. Maisch, Germany) mated to a metal emitter in-line with an Orbitrap Elite (Thermo Scientific, USA). The mass spectrometer was operated in data dependent mode with the 120,000 resolution MS1 scan (400–1800 m/z) in the Orbitrap followed by up to 20 MS/MS scans with collision-induced dissociation fragmentation in the ion trap. A dynamic exclusion list was invoked to exclude previously sequenced peptides for 120 s if sequenced within the last 30 s and maximum cycle time of 3 s was used.

Raw files were searched using MS-Amanda (Bern et al. 2012) and Sequest HT algorithms (Eng et al. 1994) within the Proteome Discoverer 2.1 suite (Thermo Scientific, USA). 15 ppm MS1 and 0.5 Da MS2 mass tolerances were specified. Carbamidomethylation of cysteine was used as a fixed modification, oxidation of methionine, and deamidation of asparagine were specified as dynamic modifications. Trypsin digestion with a maximum of 2 missed cleavages was allowed. Files were searched against the *Saccharomyces* genome database (SGD) downloaded 2015 January 13 and supplemented with common contaminants.

Scaffold (version Scaffold\_4.7.5, Proteome Software Inc., Portland, OR) was used to validate MS/MS-based peptide and protein identifications. Peptide identifications were accepted if they could be established at greater than 95.0% probability by the scaffold local false discovery rate algorithm. Protein identifications were accepted if they could be established at greater than 99.9% probability and contained at least 2 identified peptides. Protein probabilities were assigned by the Protein Prophet algorithm (Nesvizhskii et al. 2003). Proteins that contained similar peptides and could not be differentiated based on MS/MS analysis alone were grouped to satisfy the principles of parsimony.

### Co-immunoprecipitation

Cells were sporulated for 4 hours as described above and a volume of cells equivalent to 25 OD units was harvested for each strain. Cells were resuspended in 200  $\mu$ l of lysis buffer (1% Triton-X 100, 0.2 M Tris-HCl pH 7.4, 0.3 M NaCl, 20% glycerol, 0.002 M ethylenediaminetetraacetic acid) supplemented with 10 $\times$  protease inhibitor (Pierce) and lysed using the FastPrep (MP) for four rounds of 40 seconds at 4.0 m/s with one minute on ice between each round of bead beating. Protein extracts were then incubated with 15  $\mu$ l of anti-MYC or anti-hemagglutinin (HA) magnetic beads (Pierce) for 1 hour at room temperature. Beads were washed three times with lysis buffer, resuspended in deionized water, and moved to a new tube before being resuspended in 2 $\times$  sample buffer and boiled for 5 minutes to elute proteins off the beads. Samples were then resolved on 8% sodium dodecyl-sulfate polyacrylamide gel electrophoresis (SDS-PAGE) and western blotting was conducted as described below.

### Western blotting

Protein samples were resolved on an appropriate percentage SDS-PAGE gel before being transferred to a polyvinylidene difluoride membrane using a semidry transfer apparatus (TransBlot SD BioRad) at 25 volts for 30 minutes. After transfer, membranes were blocked for 30 minutes using 10% milk in TBS before being incubated with primary antibody (anti-HA (12CA5) 1:1,000,

anti-HA (rabbit: Cell Signaling C29F4) 1:2,500, anti-MYC (9E10) 1:1,000, anti-MYC (rabbit: Novus NB600-336SS) 1:1,000, anti-FLAG (Sigma M2) 1:1,000, anti-green fluorescent protein (GFP) (BD Living Colors 632377) 1:1,000, anti-PGK1 (Invitrogen 22C5D8) 1:1,000) for 1 hour at room temperature. Membranes were then washed three times for ten minutes each with 0.1% TBS-Tween20 (TBST) before being incubated with the appropriate secondary antibody in 1% milk in TBST for 30 minutes at room temperature. Incubation with secondary antibody (donkey anti-mouse IgG (Jackson ImmunoResearch) 1:10,000 or donkey anti-rabbit IgG (ImmunoResearch) 1:20,000) was then followed by one brief rinse in TBST and another three washes for ten minutes each with TBST before being incubated with Immobilon Western horse radish peroxidase substrate (Millipore) for 5 minutes and imaged using the G-Box from SynGene. Densitometry was conducted using ImageJ.

### Protein extraction

Proteins were extracted as previously described (Park, Sporer, et al. 2023). Samples were incubated with 150  $\mu$ l of 1.85 M NaOH on ice for 10 minutes. 150  $\mu$ l of 50% trichloroacetic acid was then added to the samples and they were left to incubate at 4°C for 10 minutes. Samples were then washed with acetone before being resuspended in 100  $\mu$ l of 2 $\times$  sample buffer. Samples were then boiled for five minutes and then kept on ice for five minutes before being spun down and moved to new tubes. Samples were then either run on an SDS-PAGE gel or stored for later use at –80°C.

### Microscopy

Microscopy was conducted as previously described (Park, Sporer, et al. 2023). Briefly, 100  $\mu$ l of a sporulated culture expressing GFP-TUB1 integrated at TUB1 (Straight et al. 1997) and SPC42-mCherry was spun down and resuspended in 10  $\mu$ l of Spo media. Cells were imaged on a DeltaVision deconvolution microscope (Applied Precision, Issaquah, WA) based on a Nikon TE200 (Melville, NY). All images were deconvolved using Applied Precision SoftWoRx imaging software. At least one hundred cells were counted in all cases, and the percentage of cells in each meiotic stage including mature spores (dyads, triads, and tetrads) was determined using the morphology of the spindle and the number of spindle pole bodies.

### Flow cytometry

Flow cytometry was conducted as previously described (Park, Sporer, et al. 2023). Cultures were induced to sporulate and at each time point measured 500  $\mu$ l of cells were pelleted and washed in dH<sub>2</sub>O. Cells were fixed in 70% ethanol and stored at –20°C for 1 hour up to several days. After fixation, cells were washed in 500  $\mu$ l 50 mM sodium citrate (pH 7.2) and incubated in 0.5 ml sodium citrate containing 0.25 mg/ml RNaseA for 2 hours at 37°C. After RNaseA treatment, 500  $\mu$ l of 8  $\mu$ g/ml propidium iodide in sodium citrate buffer was added to each sample and incubated overnight in the dark at 4°C. The cells were then sonicated at 50% duty cycle, output setting 3, for 4 $\times$  12 pulses on ice. Fluorescence-activated cell sorting was conducted at the Flow Cytometry and Cell Sorting Shared Resource core at Georgetown University and data were analyzed using FCS Express.

### mRNA m<sup>6</sup>A methylation

mRNA methylation levels were measured as previously described (Park, Sporer, et al. 2023). SK1 cultures were sporulated for four hours. Cells were lysed using the FastPrep (MP) as described above. Total RNA was then harvested using the Qiagen RNeasy

kit with on-column DNase treatment. mRNA was purified from these total RNA samples using Oligod(T) magnetic beads (ThermoFisher). mRNA methylation was measured using the EpiQuik fluorometric m<sup>6</sup>A RNA methylation quantification kit (EpiGenTek). The kit protocol was followed as written. Briefly, purified mRNA was bound to wells and then washed before the addition of an antibody to m<sup>6</sup>A. Wells were then washed again before the addition of a detection antibody followed by an enhancer/developer solution. The fluorescence was measured using a Synergy plate reader (BioTek) at 530<sub>EX</sub>/590<sub>EM</sub> nm and m<sup>6</sup>A levels were quantified for each sample using a standard curve generated from a positive control provided with the kit. Measurements from an *ime4Δ/Δ* strain were used to subtract background from the data collected from the *vir1Δ/Δ* mutant.

### RNA-seq

RNA-seq was conducted as previously described (Park, Remillard, et al. 2023). Cells were lysed and RNA was purified as described above. RNA samples were sent to Novogene Corporation for library prep and mRNA sequencing using an Illumina-based platform (PE150). Resulting data were analyzed using the open-access Galaxy platform (Afgan et al. 2018). Reads were first mapped to the yeast genome (*sacCer3*) using the standard settings using the burrows-wheeler alignment – maximal exact match program and then counted using *htseq-count*. Differential expression analysis was conducted using DESeq2 and heat maps were made using Cluster 3.0 and Java Tree View. GO-term analysis was conducted using Yeasttract (Teixeira et al. 2014).

### qPCR

qPCR was conducted as previously described (Park, Sporer, et al. 2023). RNA was harvested as described above. cDNA libraries were constructed using the High-Capacity cDNA Reverse Transcription kit (Applied Biosystems) with 10 μl of the total RNA sample. The concentration of the resulting cDNA was measured using a nanodrop. qPCR reactions were set up using Power SYBR Green PCR Master Mix (Applied Biosystems) with 50 ng of total RNA. The reactions were run on a CFX96 Real-Time System (BioRad) with reaction settings exactly as described in the master mix instructions with the only change being the addition of a melt curve at the end of the program. Results were analyzed using CFX Maestro. Primer sequences were as follows: PGK1 Forward 5'-CTCACTTCTATGGTCGCTTTC-3', PGK1 Reverse 5'-AATGGTCTGGTTGGGTTCTC-3', IME1 Forward 5'-ATGGCAACTGGTCTGAAAG-3', and IME1 Reverse 5'-GGAACGTAGATGCGGATTCAT-3'.

### Protein fold similarity predictions

Alpha Fold structure prediction files for Vir1p (AF-P53185) and VIRMA from humans (AF-Q69YN4), *Arabidopsis* (AF-F4J8G7), and *Drosophila* (AF-Q9W1R5) were downloaded from UniProt. The downloaded pdb files were uploaded to the DALI or RaptorX DeepAlign web-based platform to conduct pairwise comparisons between Vir1p and the different versions of VIRMA. Standard input settings were used for all comparisons and the whole protein sequence was used for the predictions.

## Results

### Vir1p interacts with Kar4p in a function specific manner

Previous work from our lab identified function-specific alleles of Kar4p that are defective either in mating or in one or both of its

**Table 1.** Top meiotic Kar4p interactors detected by IP-MS.

Protein	Kar4p enrichment	Log <sub>2</sub> normalization	P-value
Mum2p	112.5	5.2	3.92E-05
Kar4p	85	4.8	1.24E-04
Ygl036wp/ Vir1p	65.5	4.5	3.38E-04
Ssa4p	43.5	3.9	1.41E-03
Sip5p	21	2.8	1.18E-02
Ime4p	15	2.3	2.63E-02

functions in meiosis (Mei and Spo). The Mei function involves Kar4p's role in mRNA methylation and the Spo function appears to involve a noncatalytic function that promotes the translation of transcripts during meiosis (Park, Remillard, et al. 2023; Park, Sporer, et al. 2023). To understand the full complement of proteins involved in mRNA methylation and Kar4p's Spo function, we conducted immunoprecipitation followed by mass spectrometry (IP-MS) to identify meiotic binding partners. We identified two known Kar4p interactors, the components of the methyltransferase complex, Ime4p, and Mum2p, as well as a heat shock protein, Ssa4p. Heat shock proteins are common contaminants of this type of experiment. The interaction with Sip5p was not confirmed (data not shown). In addition, we detected a robust interaction with a previously uncharacterized protein called Ygl036wp (Table 1). High-throughput studies had also reported the interaction between Ygl036wp and Kar4p, as well as between Ygl036wp and Mum2p (Ito et al. 2001; Gavin et al. 2002; Yu et al. 2008). Using epitope-tagged versions of Ygl036wp and Kar4p, we confirmed the interaction between the two proteins by co-immunoprecipitation (Fig. 1a, Supplementary Fig. 1).

With the interaction between Ygl036wp and Kar4p validated, we next asked if the two proteins engage in a function-specific interaction, as was seen for other members of the complex (Park, Sporer, et al. 2023). Co-immunoprecipitation (Co-IP) was used to assess the interaction between Ygl036wp and the previously identified alleles of Kar4p. Most of the Kar4p alleles that retain meiotic function (blue) maintain the interaction with Ygl036wp, except for C127Y and F186S which have a weak interaction (Fig. 1a). Most alleles with defects in meiosis show reduced interaction. Remarkably, the pattern of interactions observed between Ygl036wp and the Kar4p mutant proteins matches perfectly the interactions seen with Mum2p, suggesting that Ygl036wp may also play an important role in mRNA methylation. In mammalian systems, the ortholog of Mum2p, WTAP, acts as a linker between the catalytic complex (METTL3/14) and accessory proteins (Horiuchi et al. 2013). These findings suggest that Mum2p may be acting similarly in yeast to bridge the catalytic components (Ime4p and Kar4p) to other components (Ygl036wp and Slz1p). Given the correlation between the interactions of Mum2p and Ygl036wp with the Kar4p alleles and work discussed below, we propose to name Ygl036wp budding yeast ortholog of *VIRMA*/Virilizer/*VIR1* (Vir1p).

### Vir1p interacts with all members of the mRNA methyltransferase complex

Given that Vir1p and Kar4p interact during meiosis when Kar4p also interacts with other members of the methyltransferase complex, and that high-throughput studies reported an interaction between Vir1p and Mum2p (Gavin et al. 2002; Yu et al. 2008), we determined whether Vir1p interacts with the other members of the

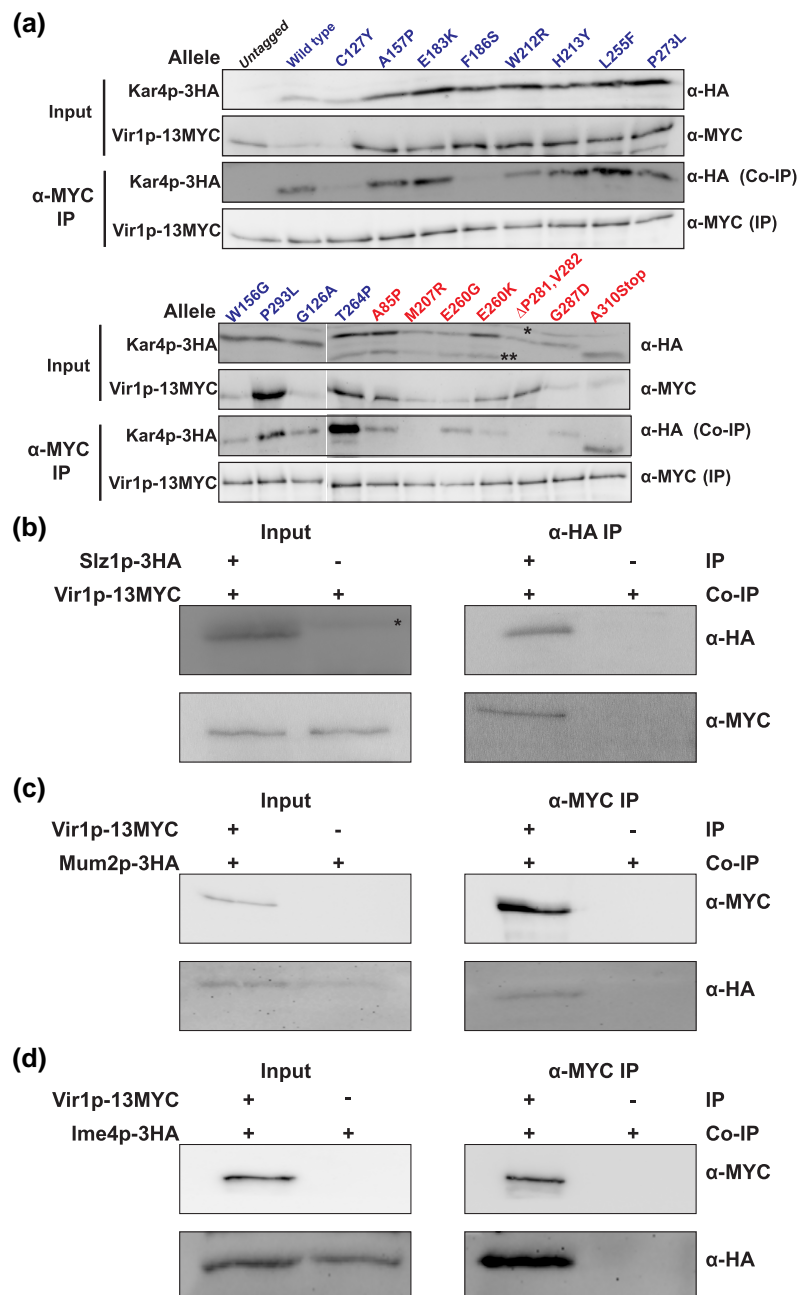


**Fig. 1.** Vir1p engages in a function specific interaction with Kar4p and interacts with all members of the mRNA methyltransferase complex. a) Western blots of total protein (Input) and Co-IPs ( $\alpha$ -MYC IP) between Vir1p-13MYC and mutant alleles of Kar4p-3HA (MY 16019). (Input) Total protein samples from the extracts that were used for the Co-IPs. “\*” indicates a nonspecific band. “\*\*\*\*” indicates degradation products of Kar4p. Note that A310Stop results in the production of a truncated protein. Alleles proficient for Kar4p’s meiotic function (Mei<sup>+</sup>) are in blue and alleles in red are not (Mei<sup>-</sup>). ( $\alpha$ -MYC IP) Co-IPs where Vir1p-13MYC was purified and the co-purification of Kar4p-3HA was assayed. Each row is derived from a single blot. One lane with an incorrect sample was cropped from the bottom set of mutation alleles. b) Western blots of total protein and Co-IPs between Slz1p-3HA and Vir1p-13MYC (MY 16408 and MY 16409). (Input) Total protein samples from the extracts that were used for the Co-IPs. “\*” indicates a nonspecific band. ( $\alpha$ -HA IP) Co-IPs where Slz1p-3HA was purified and the co-purification of Vir1p-13MYC was assayed. c) and d) Western blots of total protein and Co-IPs between Mum2p-3HA (MY 16232 and MY 16236) or Ime4p-3HA (MY 16327 and MY 16328) and Vir1p-13MYC. (Input) Total protein samples from the extracts that were used for the Co-IPs. ( $\alpha$ -MYC IP) Co-IPs where Vir1p-13MYC was purified and the co-purification of either Mum2p-3HA or Ime4p-3HA was assayed.

methyltransferase complex. By Co-IP, we found that Vir1p binds to all other previously known members of the methyltransferase complex (Slz1p, Mum2p, and Ime4p) (Fig. 1b–d).

### Vir1p is required for mRNA methylation

Vir1p’s interaction with most of the known mRNA methyltransferase complex members suggested that it might have a role in mRNA methylation. To increase the synchrony and efficiency of

meiosis we examined m<sup>6</sup>A in the SK1 strain background (Bodi et al. 2010; Agarwala et al. 2012; Schwartz et al. 2013; Bodi et al. 2015; Bushkin et al. 2019), in which we introduced a *vir1Δ/Δ* mutation. Bulk mRNA m<sup>6</sup>A methylation was measured after four hours in sporulation media, which had been previously shown to be when m<sup>6</sup>A levels peaked (Park, Sporer, et al. 2023). As expected, m<sup>6</sup>A levels were highly reduced in *vir1Δ/Δ* (Fig. 2a), similar to *ime4 Δ/Δ*.

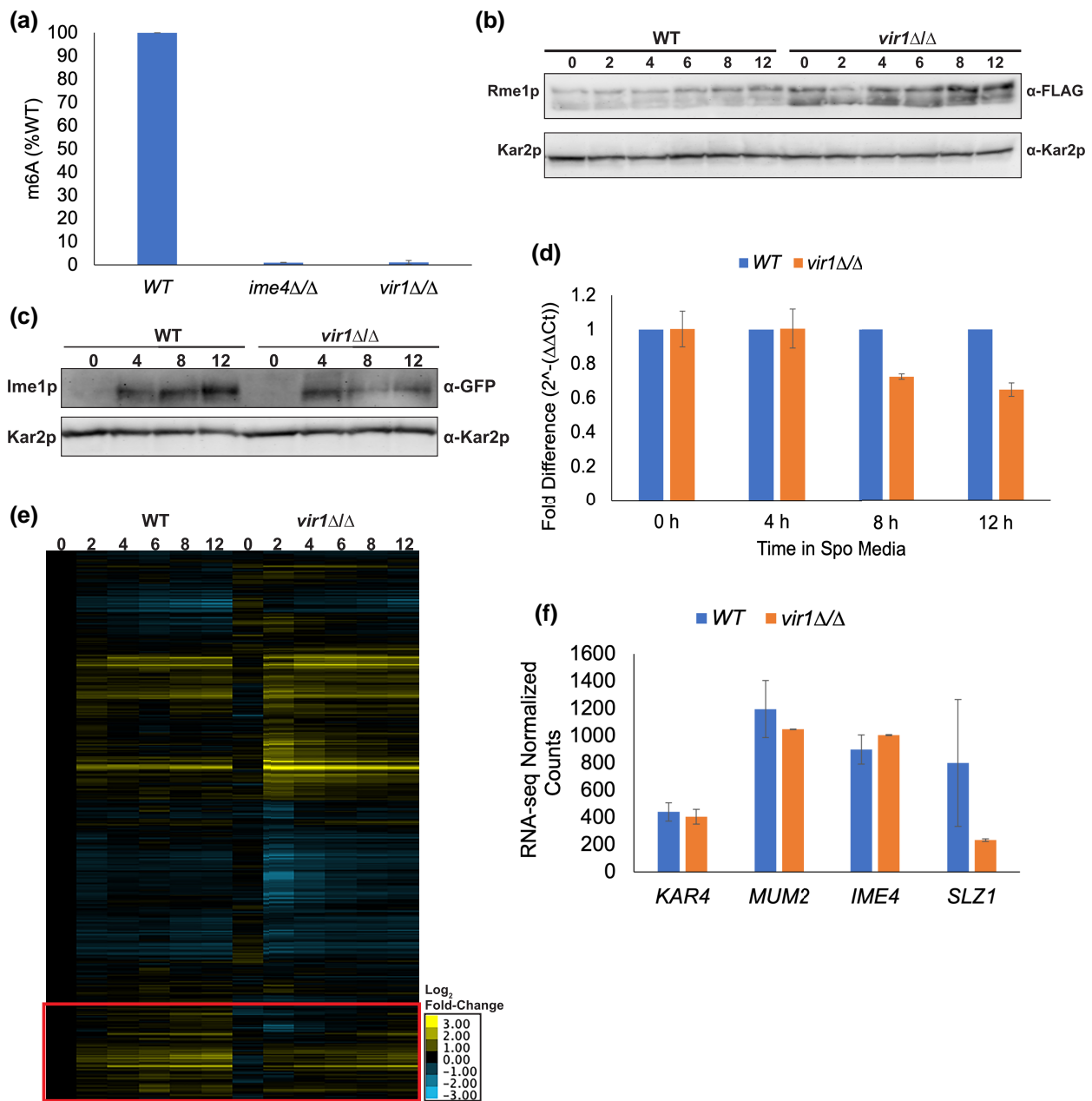


**Fig. 2.** Vir1p is required for mRNA m<sup>6</sup>A methylation. a) mRNA m<sup>6</sup>A levels measured using an enzyme-linked immunosorbent assay from EpiGenTek. The indicated mutations were made in the SK1 strain background (MY 16325, MY 16326, and MY 16369) and samples were harvested after 4 hours of exposure to meiosis-inducing conditions. Experiments were run in three biological replicates for each strain and error bars represent standard deviation. b) Western Blot of 3xFLAG-Rme1p in wild type (MY 16563) and *vir1*ΔΔ (MY 16575) across a time course of meiosis. Kar2p is used as a loading control. c) Western blot showing GFP-Ime1p levels across a time course of meiosis in wild type (MY 16550) and *vir1*ΔΔ (MY 16574). Kar2p is used as a loading control. d) qPCR measuring *IME1* transcript levels in wild type and *vir1*ΔΔ. Data were normalized to levels of *PGK1* expression. Error bars are SEM of three biological replicates. e) Heatmap of RNA-seq data across a time course of meiosis (0, 2, 4, 6, 8, and 12 hours) in wild type (MY 16616) and *vir1*ΔΔ (MY 16618). An S-phase population first appears at 12 hours in these strains. Expression was normalized to wild type pre-induction of sporulation (t = 0). Genes were clustered in Cluster3.0 and the heatmaps were constructed with Java TreeView. The boxed region demarcates clusters of genes with delayed and reduced expression in *vir1*ΔΔ.

Loss of mRNA methylation has been shown to increase levels of the negative regulator of *IME1*, Rme1p. Using an epitope-tagged version of Rme1p, Rme1p levels were increased at least 2-fold in *vir1*ΔΔ compared to wild type across the time course of meiosis (Fig. 2b). Consistent with increased Rme1p levels, there was a ~2-fold decrease in the level of *IME1* transcript and protein in *vir1*ΔΔ at 8 and 12 hours in meiosis-inducing conditions (Fig. 2c and 2d). This is consistent with work that has shown there is an early burst of *IME1* expression that is m<sup>6</sup>A independent, but that

sustained induction of *IME1* requires mRNA methylation (Bushkin et al. 2019).

The mis-regulation of *IME1* expression suggested that there should be defects in the meiotic transcriptome of *vir1*ΔΔ. Using RNA-seq across the time course of meiosis in wild type and *vir1*ΔΔ, we saw that the transcript profiles were quite similar (Fig. 2e). However, a cluster of genes show delayed and reduced expression in the mutant relative to wild type (Fig. 2e). To confirm that the impacted genes are involved in meiosis, we did a pairwise

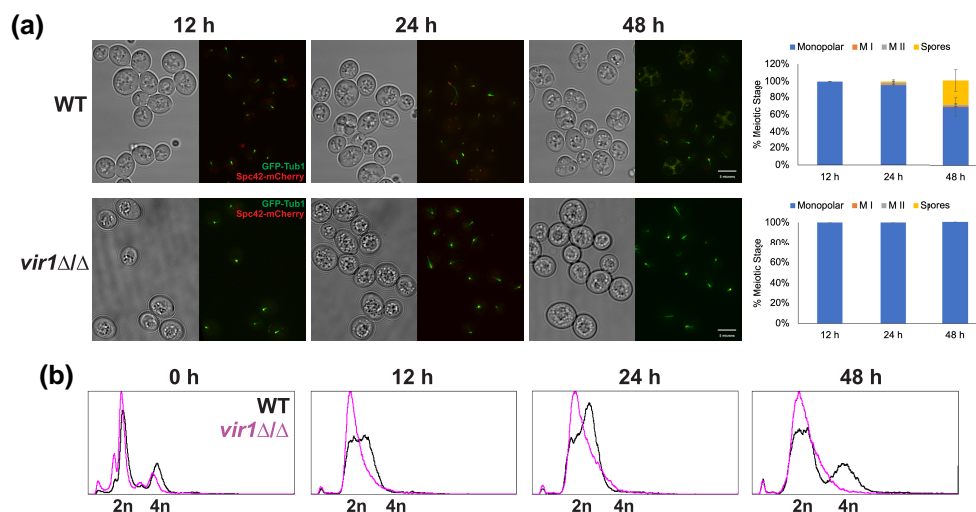


**Fig. 3.** Vir1p is required early in meiosis. a) Fluorescence microscopy of the spindle pole body (Spc42p-mCherry) and microtubules (GFP-Tub1p) across a time course of meiosis (12, 24, and 48 hours post transfer into sporulation media) in wild type (MY 16294) and *vir1Δ/Δ* (MY 16365). Graphs show quantification of the number of cells in different meiotic stages (Monopolar Spindle, Meiosis I, Meiosis II, and Spores). Experiments were run in three biological replicates for each strain and at least 100 cells were counted for each replicate. Error bars represent standard deviation. b) Flow cytometric analysis of DNA content in wild type (MY 16616) and *vir1Δ/Δ* (MY 16618) across the same meiotic time course of the microscopy. DNA was stained with propidium iodide.

comparison to determine differentially expressed genes between wild type and *vir1Δ/Δ* at each time point analyzed. Interestingly, at 2 hours many genes involved in translation and ribosome biogenesis are down regulated in *vir1Δ/Δ*. The reason for this reduction is unclear and warrants further investigation into a potential role for mRNA methylation in the response to glucose starvation alone. Looking specifically at genes with a 2-fold or greater defect at 4 hours in *vir1Δ/Δ*, which is when a gene expression defect becomes noticeable on the heat map, GO-term analysis revealed a specific defect in meiotic progression (Fig. 2e red box). Of the 73 genes reduced at 4 hours, the top three GO-terms were “biological process” ( $P = 0.05$ ), “meiotic cell cycle” ( $P = 5.2 \times 10^{-7}$ ), and “reciprocal meiotic recombination” ( $P = 4.3 \times 10^{-8}$ ). The reduction in early meiotic gene expression is consistent with increased Rme1p and decreased Ime1p levels observed in *vir1Δ/Δ* (Fig. 2, b and 2c). There was no impact on the expression of other methyltransferase complex members in *vir1Δ/Δ* except for SLZ1 (Fig. 2f). This is expected given that SLZ1 expression is Ime1p dependent. Together, these data support Vir1p being a member of the mRNA methyltransferase complex and important for the regulation of genes required early in meiosis including IME1.

### *vir1Δ/Δ* mutants arrest early in meiosis

The loss of m<sup>6</sup>A and reduction in Ime1p in *vir1Δ/Δ* suggested that *vir1Δ/Δ* mutants would be unable to sporulate and should arrest early in meiosis before premeiotic DNA synthesis. Using wild type and *vir1Δ/Δ* strains expressing GFP-TUB1 and SPC42-mCherry, we used fluorescence microscopy to track meiotic progression (Fig. 3a). Wild-type strains progressed through both meiotic divisions and reached ~30% sporulation by 48 hours after induction. In contrast, *vir1Δ/Δ* mutants were arrested with a monopolar spindle and do not progress to sporulation (Fig. 3a). To assess the ability of these strains to undergo premeiotic DNA synthesis, we used flow cytometry to measure DNA content. Wild-type strains began replicating DNA by 12 hours and contained a distinct 4N population by 48 hours. The *vir1Δ/Δ* mutants did not initiate premeiotic DNA synthesis and remained arrested

at 2N (Fig. 3b). This early arrest phenotype is consistent with a role for Vir1p in regulating meiotic entry via mRNA methylation.

### Loss of Rme1p and IME1 overexpression partially suppresses the *vir1Δ/Δ* meiotic defect

RME1 transcripts are one of the key targets of mRNA methylation and methylation leads to their rapid turnover (Bushkin et al. 2019). Strains lacking either Kar4p or Ime4p in which Rme1p levels are reduced or absent do progress through premeiotic DNA synthesis, but do not complete meiosis and spore formation (Bushkin et al. 2019; Park, Sporer, et al. 2023). Suppression of Kar4p’s Mei function by loss of Rme1p was due to the restoration of normal levels of IME1 expression (Park, Sporer, et al. 2023). Given that Vir1p also appears to be working in this same pathway, we asked if a *vir1Δ/Δ rme1Δ/Δ* double mutant could undergo premeiotic DNA synthesis. By flow cytometry, otherwise wild-type strains lacking Rme1p began to form a 4N population faster than in strains with Rme1p. As expected for mutations in the methyltransferase complex, *vir1Δ/Δ rme1Δ/Δ* double mutants underwent premeiotic DNA synthesis. However, these strains still failed to sporulate (Fig. 4a and Supplementary Fig. 2).

Given that loss of the negative regulator of IME1, Rme1p, partially suppressed the *vir1Δ/Δ* meiotic defect, we asked directly if overexpression of IME1 also suppressed, as it does with *kar4Δ/Δ* (Park, Remillard, et al. 2023; Park, Sporer, et al. 2023). IME1 was overexpressed using the estradiol inducible P<sub>Z3EV</sub> promoter system (Pzev) (McIsaac et al. 2014). Wild-type strains sporulated very efficiently after IME1 overexpression, reaching 86% sporulation by 48 hours. However, 93% of the *vir1Δ/Δ* mutants were arrested with a monopolar spindle; only 6% formed spores after IME1 overexpression (Fig. 4b). As in *kar4Δ/Δ*, IME1 overexpression permitted premeiotic DNA synthesis in *vir1Δ/Δ*, more robustly than the *vir1Δ/Δ rme1Δ/Δ* double mutant (Fig. 4c). This suggests that loss of Rme1p can facilitate some level of meiotic entry in *vir1Δ/Δ*, but either the level of Ime1p is insufficient or there are still other factors inhibiting the mutant. The requirement for these other factors is only fully bypassed upon the direct overexpression of IME1.

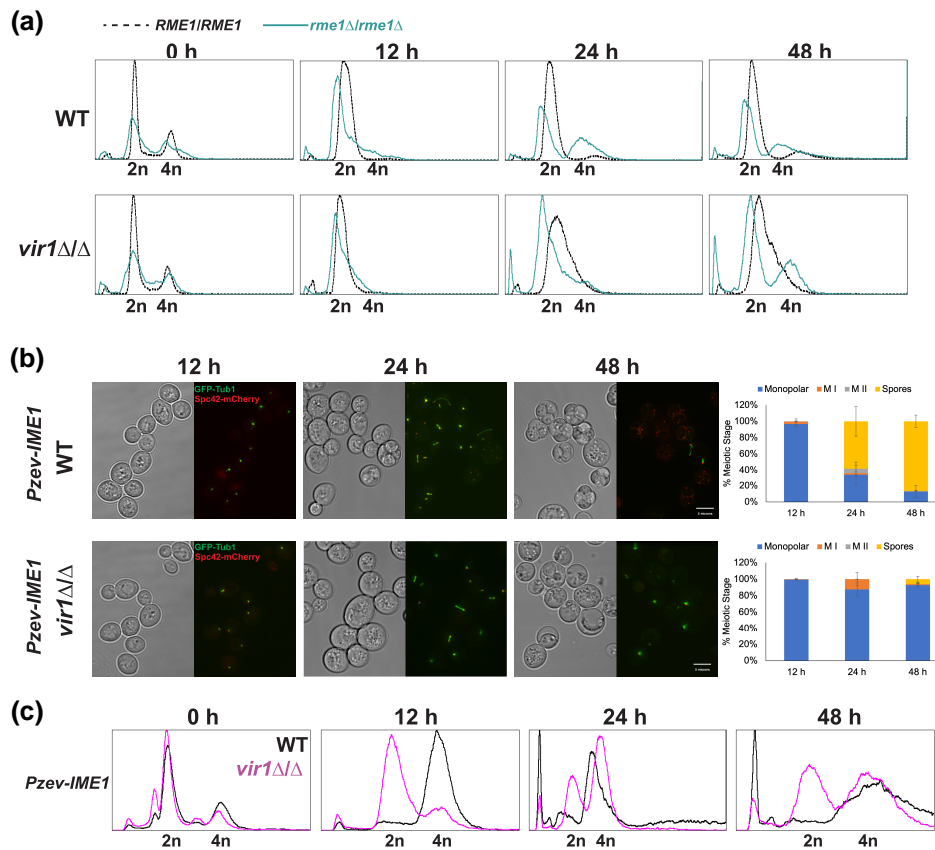


**Fig. 4.** Loss of Rme1p and overexpression of *IME1* partially rescues the *vir1Δ/Δ* meiotic defect. a) Flow cytometric analysis of DNA content in wild type and *vir1Δ/Δ* carrying the wild type allele of *RME1* (MY 16616 and MY 16618) or a deletion of *RME1* (MY 16456 and MY 16609) across a time course of meiosis. DNA was stained with propidium iodide. b) Fluorescence microscopy of the spindle pole body (Spc42p-mCherry) and microtubules (GFP-Tub1p) across a time course of meiosis (12, 24, and 48 hours post movement into sporulation media) in wild type (MY 16294) and *vir1Δ/Δ* (MY 16365) with *IME1* overexpressed from an estradiol-inducible promoter. Graphs are the quantification of the number of cells in different meiotic stages (Monopolar Spindle, Meiosis I, Meiosis II, and Spores). Experiments were run in three biological replicates for each strain and at least 100 cells were counted for each replicate. 1  $\mu$ M of estradiol was used to induce expression. Error bars represent standard deviation. c) Flow cytometric analysis of DNA content in wild type (MY 16534) and *vir1Δ/Δ* (MY 16293) with *IME1* overexpressed across the same meiotic time course of the microscopy. DNA was stained with propidium iodide.

To understand the lack of sporulation after *IME1* overexpression in *vir1Δ/Δ*, we used RNA-seq to look at the transcriptome. The overexpression of *IME1* revealed later transcript level defects in both the expression of the middle meiotic transcription factor, *NDT80*, and *Ndt80p*-dependent genes (Fig. 5a (red box) and Fig. 5b). Some 58% of the genes highlighted by the red box in Fig. 5a were found to be regulated by *Ndt80p*. This finding is consistent with data for *kar4Δ/Δ* after *IME1* overexpression, indicating that the block in meiosis after *IME1* overexpression in *vir1Δ/Δ* is also upstream of *NDT80* expression (Park, Remillard, et al. 2023). Loss of Rme1p (Bushkin et al. 2019) and *IME1* overexpression alone (Park, Sporer et al. 2023) can rescue the meiotic defect of a catalytically dead mutant of *Ime4p*, suggesting that remaining defects after overexpression of *IME1* do not involve mRNA methylation. Thus, Vir1p may also be involved in the potential noncatalytic function of the complex.

### ***IME1* and *RIM4* overexpression suppresses the *vir1Δ/Δ* meiotic defect**

The co-overexpression of *IME1* and the translational regulator, *RIM4*, fully suppresses the meiotic defect of *kar4Δ/Δ*, *mum2Δ/Δ*, and *ime4Δ/Δ* (Park, Remillard, et al. 2023; Park, Sporer, et al. 2023). Given the similarities between these mutants and *vir1Δ/Δ*, we tested whether *IME1* and *RIM4* co-overexpression also fully

rescues the *vir1Δ/Δ* meiotic defect. Using strains with both *Pzev-IME1* and *Pzev-RIM4*, wild-type strains sporulate more efficiently with either or both genes overexpressed (Fig. 5c). The *vir1Δ/Δ* mutant also sporulated after co-overexpression, but not as efficiently, and delayed by 24-hours compared to wild type, suggesting that defects persist in this strain (Fig. 5c and Supplementary Fig. 3). However, co-overexpression did restore *vir1Δ/Δ* to roughly the same level and timing of sporulation as wild type strains with *RIM4* overexpressed (Fig. 5c and Supplementary Fig. 3). To understand why there is still a delay in sporulation after *IME1* and *RIM4* co-overexpression, we again used RNA-seq this time looking at later time points (24 and 48 hours). Even with co-overexpression, there was a pronounced delay in *NDT80* expression in *vir1Δ/Δ*, as was seen in *kar4Δ/Δ* under the same conditions (Fig. 5b) (Park, Remillard, et al. 2023). The persistent delay in *NDT80* expression explains the delayed and inefficient sporulation in *vir1Δ/Δ*.

### **Vir1p is required for efficient expression of multiple meiotic proteins**

The requirement for *RIM4* overexpression for the completion of meiosis suggested that *vir1Δ/Δ* mutants, like *kar4Δ/Δ* mutants, would have defects in the levels of key meiotic proteins (Park, Remillard, et al. 2023). The level of the meiotic kinase *Ime2p* was



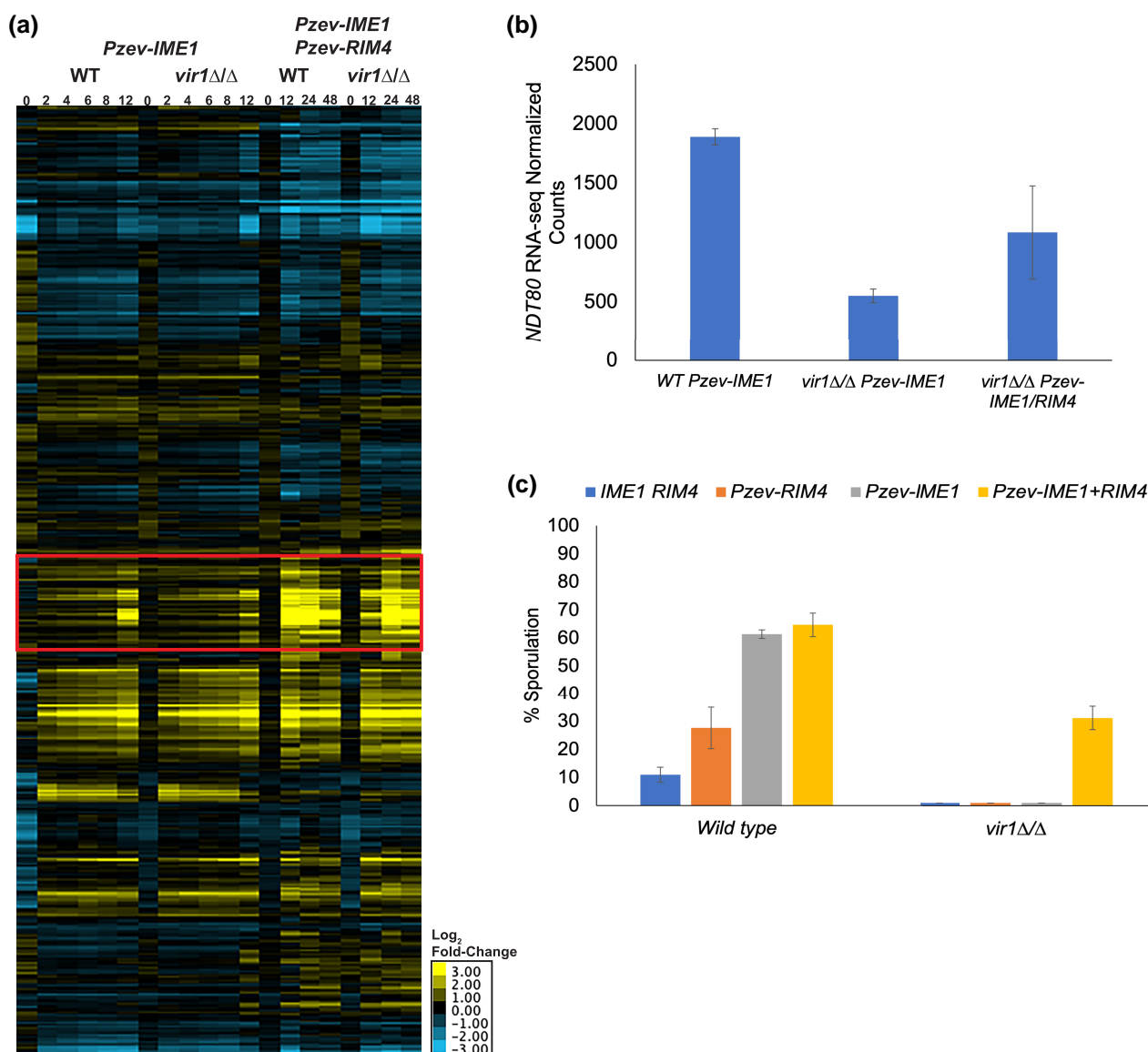


**Fig. 5.** Co-overexpression of *IME1* and *RIM4* rescues the *vir1Δ/Δ* meiotic defect. a) Heatmap of RNA-seq data across a time course of meiosis in wild type (MY 16534) and *vir1Δ/Δ* (MY 16293) with *IME1* overexpressed (0, 2, 4, 6, 8, and 12 hours) and in wild type (MY 16533) and *vir1Δ/Δ* (MY 16073) with *IME1/RIM4* co-overexpressed (0, 12, 24, and 48 hours). Expression was normalized to wild type  $t = 0$  used in Fig. 2. Genes were clustered in Cluster3.0 and the heatmaps were constructed with Java TreeView. The boxed region demarcates a cluster of genes with delayed and reduced expression in *vir1Δ/Δ*. b) *NDT80* RNA-seq normalized counts from wild type and *vir1Δ/Δ* with *IME1* overexpressed and from *vir1Δ/Δ* with *IME1* and *RIM4* overexpressed. Counts were normalized using the standard normalization method in DESeq2. Error bars represent standard deviation between two biological replicates. c) Sporulation of wild type and *vir1Δ/Δ* with either endogenous expression of *IME1* and *RIM4* (MY 16616 and MY 16618), overexpression of *IME1* (MY 16532 and MY 16077), overexpression of *IME1* (MY 16534 and MY 16293), or overexpression of both *IME1* and *RIM4* (MY 16533 and MY 16073). 1  $\mu$ M of estradiol was used to induce expression. All dyads, triads, and tetrads were counted across three biological replicates for each strain. At least 100 cells were counted after 48 hours post addition of estradiol. Error bars represent standard error of three biological replicates.

not reduced in *kar4Δ/Δ* with endogenous *IME1* expression, indicating that *Ime2p* is not limiting the progression of *kar4Δ/Δ* mutants through the early stages of meiosis (Park, Remillard, et al. 2023). However, after overexpression of *IME1* in *kar4Δ/Δ*, the level of *Ime2p* was found to be reduced later in meiosis, compared to wild type (Park, Remillard, et al. 2023). In *vir1Δ/Δ* mutants without *IME1* overexpression, *IME2* transcript levels were reduced about 2-fold, but *Ime2p* levels were normal (Supplementary Fig. 4). The reduction in *IME2* transcript is consistent with the reduction in *Ime1p* expression, although the lack of an effect on the level of the protein is surprising. After *IME1* overexpression, there was a ~2-fold reduction in *IME2* transcript and a similar reduction in *Ime2p* levels in *vir1Δ/Δ* (Fig. 6a and 6b), similar to *kar4Δ/Δ*.

Co-overexpression of *IME1* and *RIM4* in *vir1Δ/Δ* both increased *Ime2p* levels and reduced the time to peak expression compared to *IME1* overexpression alone (Fig. 6c). It is likely that the delay in *NDT80* expression in *vir1Δ/Δ* after *IME1* overexpression (Fig. 5b) leads to the loss of the late induction of *IME2* expression, as previously reported in *NDT80* mutants (Shin et al. 2010).

Mass spectrometry of the meiotic proteome with *IME1* overexpressed revealed other proteins with low levels in *kar4Δ/Δ*, including the midlate meiotic proteins *Gas4p* and *Sps2p* (Park, Remillard, et al. 2023). Similarly, in *vir1Δ/Δ*, *GAS4* and *SPS2* transcript and protein levels were very low after *IME1* overexpression compared to wild type (Fig. 6d and 6e). Overexpression of *IME1* and *RIM4* only slightly increased transcript levels but caused a large

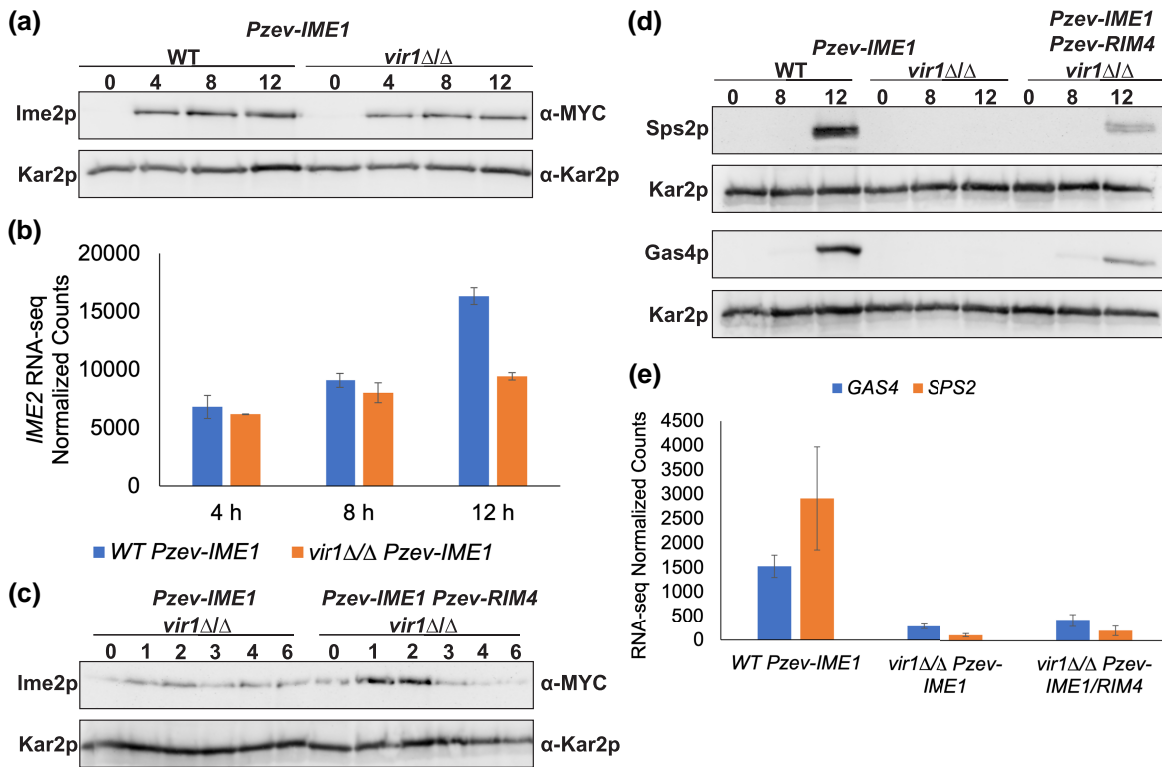


**Fig. 6.** Vir1p is required for the full expression of Ime2p, Sps2p, and Gas4p. a) Western blots of Ime2p-13MYC across a meiotic time course in wild type (MY 16608) and *vir1ΔΔ* (MY 16611) with *IME1* overexpressed. Kar2p is used as a loading control. b) *IME2* RNA-seq counts normalized between wild type (MY 16534) and *vir1ΔΔ* (MY 16293) with *IME1* overexpressed. Counts were normalized using the standard normalization method in DESeq2. Error bars represent standard deviation between two biological replicates. c) Western blots of Ime2p-13MYC across a time course of meiosis in *vir1ΔΔ* with either *IME1* overexpressed (MY 16611) or *IME1* and *RIM4* overexpressed (MY 16628). Kar2p is used as a loading control. d) Western blots of Sps2p-3HA and Gas4p-3HA in wild type (MY 16209 and MY 16208) and *vir1ΔΔ* (MY 16215 and MY 16219) with *IME1* overexpressed and in *vir1ΔΔ* with *IME1* and *RIM4* overexpressed (MY 16292 and MY 16371). Blots in the same row were exposed for the same length of time. Kar2p serves as a loading control. e) *SPS2* (Top) and *GAS4* (Bottom) RNA-seq normalized counts from 12-hour time points in wild type with *IME1* overexpressed (MY 16534) and *vir1ΔΔ* with either *IME1* overexpressed (MY 16293) or *IME1* and *RIM4* overexpressed (MY 16073). Counts were normalized using the standard normalization method in DESeq2. Error bars represent standard deviation between two biological replicates.

increase in protein levels. The persistent delay in *NDT80* expression explains the low transcript and protein levels of *GAS4* and *SPS2*, given that they are Ndt80p-dependent genes (Fig. 5b, Fig. 6d and 6e). Nevertheless, overexpression of Rim4p greatly increased the levels of both Gas4p and Sps2p. Rim4p was first identified as an early activator of meiotic gene expression, which may be related to the increased levels of Gas4p and Sps2p levels. Thus, in *vir1ΔΔ*, as in *kar4ΔΔ*, defects in the expression of proteins upstream of *NDT80* effect the expression of proteins needed later in the meiotic program (Park, Remillard, et al. 2023), which are not rescued by overexpressing *IME1*. Taken together, these data show that Vir1p behaves like other methyltransferase complex members by affecting regulation both upstream and downstream of Ime1p.

### Vir1p is the yeast homolog of VIRMA/virilizer/VIR

Given the high degree of conservation between the core components of the mRNA methyltransferase complex in eukaryotes, we asked if there are also homologs of Vir1p. Vir1p is highly conserved amongst the ascomycetes, however, no obvious homologs were found in outgroups. Vir1p has several predicted disordered regions suggesting that the selection on maintaining the primary amino acid sequence is not as strong (Supplementary Fig. 5a). However, remote homologs have been identified that share structure and function but are not strongly conserved at the primary amino acid sequence (Holm 2022). The yeast homologs of many

components of the methyltransferase complex in other eukaryotes including METTL3 (Ime4p), METTL14 (Kar4p), WTAP (Mum2p), and Z3CH13 (Slz1p) are already known. There are only three other members of the complex that have been identified in eukaryotes thus far: HAKAI, RMB15/15B, and VIRMA/Virilizer/VIR. The Alpha Fold predictions of Vir1p, were compared to the predicted structures of the three proteins that have yet to be shown to have a yeast homolog. Of the three, the predicted structure of Vir1p was strongly similar to that of VIRMA/Virilizer/VIR.

To quantify the similarities in the predicted structures, we used the DALI program (Holm 2022) to determine if Vir1p is predicted to fold like VIRMA. Although VIRMA and related proteins are much larger than Vir1p, and Vir1p lacks an N-terminal beta-pleated sheet domain, there is a core region of all that shares similar predicted structure, whether between Vir1p and human VIRMA (Fig. 7a blue region), plants (VIR) (Fig. 7b blue region), or flies (Virilizer) (Fig. 7c blue region). The similarity to Virilizer was the highest, with a Z-score of 13.9 and an root mean square deviation (RMSD) of 10.1. Comparing Virilizer and VIR to VIRMA resulted in comparable statistics; Virilizer had a Z-score of 24.5 and RMSD of 5.4, while VIR had a Z-score of 14.4 and RMSD of 14.4. The VIRMA-like proteins from all three organisms shared about 10% identity to Vir1p. Similarly, the RaptorX DeepAlign program (Kallberg et al. 2012) identified the same region of conserved structure between the VIRMA homologs and Vir1p (Fig. 7 third column highlighted regions). Again, Virilizer had the strongest match to

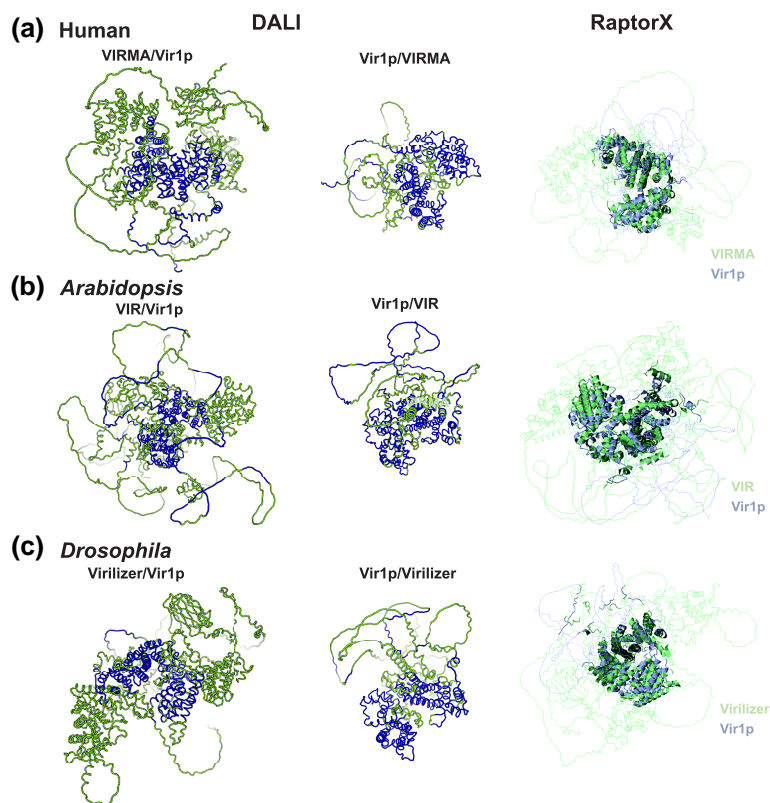


**Fig. 7.** Vir1p is the yeast homolog of VIRMA/Virilizer/VIR. Dali predictions of conserved structure between Vir1p and VIRMA from a) humans, b) *Arabidopsis*, and c) *Drosophila*. (Left) Image of the AlphaFold predicted structure of VIRMA (green) with the DALI determined region conserved with Vir1p highlighted in blue. (Center) Image of the AlphaFold predicted structure of Vir1p (green) with the DALI determined region conserved with VIRMA highlighted in blue. The Z-score for each comparison was well above the Z-score of 2, which would be considered spurious similarity. (Right) RaptorX predictions of conserved structure between Vir1p and VIRMA. Highlighted regions of Vir1p (blue) and VIRMA (green) indicate regions of the two proteins that were predicted to have similar structure.

Vir1p with an RMSD of 5.63 and a template modeling (TM) score of 0.426.

Interestingly, Blastp revealed conserved motifs located in the disordered C-terminal region of Vir1p (Supplementary Fig. 5b). DEPICTER (Barik et al. 2020), which computationally predicts the functions of intrinsically disordered domains, strongly predicts that the C-terminal disordered region of Vir1p is involved in DNA binding and protein–protein interaction, and less strongly in RNA binding. It is tempting to speculate that Vir1p’s disordered C-terminus may function to anchor the complex to chromatin while it methylates mRNA. Published data suggests that other complex members do not associate with chromatin (Ensinck et al. 2023). Thus, it is more likely that Vir1p’s disordered regions are important for facilitating protein–protein interactions.

### Vir1p is required for the stability of the mRNA methyltransferase complex

A second requirement for identifying proteins with remote homology is that they share similar functions. Research on VIRMA suggests that it acts to stabilize other complex members including WTAP (Yue et al. 2018). If Vir1p is a remote homolog of VIRMA, then Vir1p should also be required for the stability of the complex. The stability of Kar4p, Mum2p, and Ime4p was measured during meiosis in *vir1Δ/Δ* using cycloheximide to block new protein synthesis. All three proteins were unstable in *vir1Δ/Δ*. The turnover rate of Kar4p was 2-fold faster in *vir1Δ/Δ* compared to wild type (Fig. 8a). Mum2p is very stable in wild type with a half-

life longer than 60 minutes, but in *vir1Δ/Δ* the half-life dropped to ~24 minutes (Fig. 8b). Ime4p was so unstable in *vir1Δ/Δ* that it could not be detected, preventing measurement of the half-life in the mutant (Fig. 8c). We did not examine the stability of Slz1p because we saw strong defects in *SLZ1* transcript levels in *vir1Δ/Δ* (Fig. 2f).

We next examined the impact of deleting other complex members on the stability of the overall complex. We previously found that Ime4p levels are not reduced in *kar4Δ/Δ* (Park, Sporer, et al. 2023). Vir1p and Mum2p levels were also not impacted in *kar4Δ/Δ* (Supplementary Fig. 6a and 6b). However, the absence of Ime4p resulted in significantly lower levels of Kar4p, and Kar4p turned over faster in *ime4Δ/Δ* (Supplementary Fig. 7a). This is further evidence that Kar4p’s role in meiosis is dependent on its interaction with Ime4p. Mum2p levels were also reduced in *ime4Δ/Δ*, and the turnover rate was slightly increased, although not to the same extent as for Kar4p (Supplementary Fig. 7b). Neither the levels of Vir1p nor its turnover were impacted in *ime4Δ/Δ* (Supplementary Fig. 7c). A concurrent paper (Ensinck et al. 2023) found that Vir1p levels were lower in *ime4Δ/Δ* in the SK1 strain background. The discrepancy is most likely due to differences in meiotic efficiency between SK1 and the S288c strain background used in this study. SK1 undergoes meiosis much more rapidly than S288c, and so the defect in Vir1p levels may arise at later points in meiosis. In *mum2Δ/Δ*, similar to the effect of *vir1Δ/Δ*, the turnover rate of Kar4p was increased though not to the same extent as in *vir1Δ/Δ* and Ime4p was not detectable

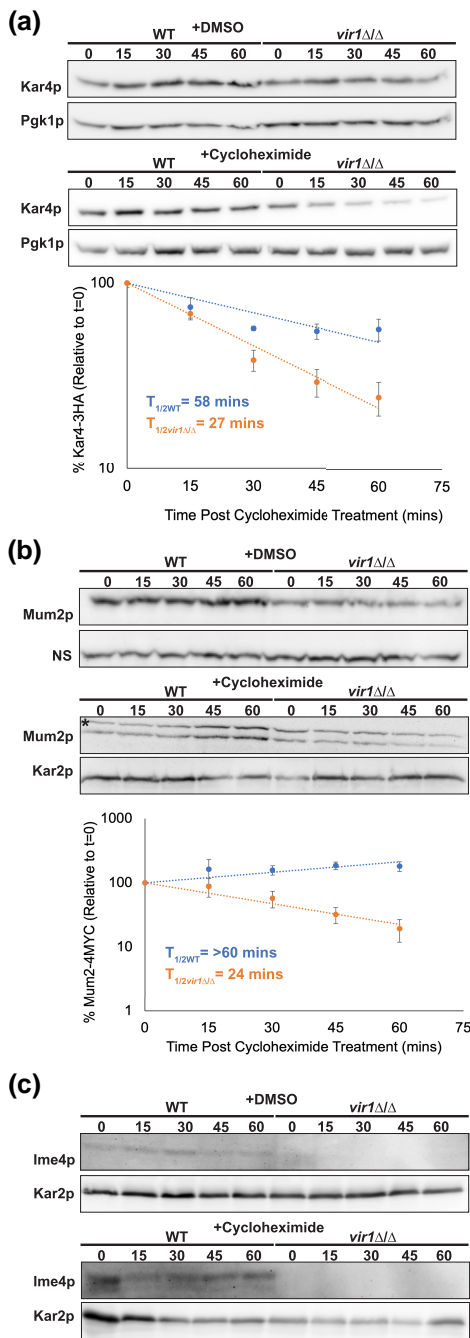


**Fig. 8.** Vir1p is required for the stability of the mRNA methyltransferase complex. a) Western blots of Kar4p-3HA after 4 hours in meiosis-inducing media with either 100  $\mu$ M cycloheximide or an equivalent amount of DMSO in both wild type (MY 16518) and *vir1Δ/Δ* (MY 16519). (Top) Kar4p-3HA levels with DMSO. (Bottom) Kar4p-3HA levels with cycloheximide. Graph is the quantification of 3 biological replicates of the cycloheximide chase experiment. Pgk1p is used as a loading control. b) Western blot of Mum2p-4MYC (bottom band) after 4 hours in meiosis-inducing media with either 100  $\mu$ M cycloheximide or an equivalent amount of DMSO in both wild type (MY 16522) and *vir1Δ/Δ* (MY 16508). (Top) Mum2p-4MYC levels with DMSO. A nonspecific band is used as a loading control (Bottom) Mum2p-4MYC levels with cycloheximide. Graph is the quantification of three biological replicates of the cycloheximide chase experiment. Kar2p is used as a loading control. “\*” indicates a nonspecific band. Error bars in A and B are SEM of the three biological replicates. c) Western blot of 3MYC-Ime4 after 4 hours in meiosis-inducing media with either 100  $\mu$ M cycloheximide or an equivalent amount of DMSO in both wild type (MY 16629) and *vir1Δ/Δ* (MY 16630). (Top) 3MYC-Ime4 levels with DMSO. (Bottom) 3MYC-Ime4 levels with cycloheximide. Kar2p is used as a loading control.

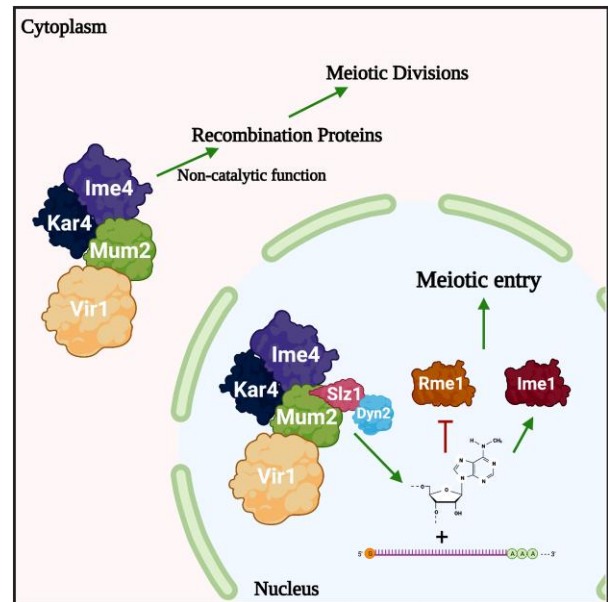


**Fig. 9.** A model for the function of Vir1p in meiosis. Vir1p functions in mRNA  $m^6A$  methylation with Ime4p, Mum2p, Kar4p, Slz1p and Dyn2p. mRNA methylation facilitates meiotic entry through regulation of Rme1p and Ime1p. Vir1p, Kar4p, Mum2p, and Ime4p engage in a function seemingly independent of  $m^6A$  catalysis that is important for the progression into the meiotic divisions. Figure was created with BioRender.com.

(Supplementary Fig. 8a and 8c). The overall level of Vir1p was slightly reduced in *mum2Δ/Δ*, but there was no impact on Vir1p's turnover rate (Supplementary Fig. 8b).

Taken together, while the removal of some complex members results in reduced levels of other members, only the removal of Vir1p increased the turnover rate of all other complex members, consistent with a scaffolding role stabilizing the methyltransferase complex. Thus, the conservation of both structure and function with VIRMA/Virilizer/VIR support Vir1p being a remote homolog of those proteins.

## Discussion

The initial characterization of the mRNA  $m^6A$  methyltransferase complex in yeast suggested that it comprised only Ime4p, Mum2p, and Slz1p (Agarwala et al. 2012). Subsequent work indicated that proteins found in the complex in other eukaryotes are conserved in yeast, such as Kar4p. Recent work from our lab (Park, Sporer, et al. 2023) and others (Ensinck et al. 2023) showed that the complex also contains Kar4p. Work presented here and by Ensinck et al. (2023) show that Vir1p, the VIRMA/Virilizer/VIR homolog, is also part of the complex. Thus, the yeast methyltransferase complex is much more highly conserved than previously thought.

Building on our findings of the role of Kar4p in meiosis, we found that Vir1p is required early in meiosis and *vir1Δ/Δ* mutants have a severe loss of mRNA  $m^6A$  methylation. The impact on the expression of *IME1* and *Ime1p*-dependent genes in *vir1Δ/Δ* provides further evidence that mRNA methylation acts upstream of *IME1* to promote meiotic entry. That *IME1* overexpression and loss of Rme1p repression only partially suppress the *vir1Δ/Δ* defect, indicates that Vir1p is also involved in other functions of the complex. The role of Vir1p in other functions is characterized

by defects in protein levels in *vir1Δ/Δ* which can be bypassed by *RIM4* overexpression. It is probable that, like Kar4p (Park, Remillard, et al. 2023), Vir1p is required for the efficient expression of proteins involved earlier in the meiotic program, including in meiotic recombination (Fig. 9). The persistent block in meiosis after *IME1* overexpression is likely due to these defects. It will be interesting to determine what exactly remains impacted in these mutants after *IME1* overexpression and whether the yeast complex utilizes a similar mechanism to enhance translation as has been shown in mammalian cells (Lin et al. 2016; Wei et al. 2022).

Utilizing the previously identified separation of function mutants of Kar4p (Park, Sporer, et al. 2023), we found that mutants that impact the interaction between Mum2p and Kar4p also impact the interaction between Vir1p and Kar4p. This suggests that in yeast, as in mammals (Horiuchi et al. 2013), Mum2p (WTAP) links the catalytic components of the complex Ime4p (METTL3) and Kar4p (METTL14) to regulatory proteins. It will be interesting to determine if the interaction between Slz1p and Dyn2p also matches this pattern. One Kar4p allele, T264P, continues to be interesting given that it is strongly defective for all Kar4p's meiotic functions, but still interacts with Vir1p, Mum2p, and Ime4p (Park, Sporer, et al. 2023). One possibility is that this allele impacts the ability of Kar4p to bind mRNA and future work will investigate that possibility. Identifying an allele that results in a fully formed complex that can't interact with mRNA could be a valuable tool for determining the underlying mechanism of the additional functions of the complex.

Work on VIRMA in mammalian cells has suggested that it plays a role in concentrating m<sup>6</sup>A around stop codons and in the 3' untranslated region (UTR) (Yue et al. 2018). However, the mechanism by which it helps confer this specificity is not well understood. The predicted functions for the disordered C-terminal domain make Vir1p an interesting candidate to determine how the methyltransferase specifically methylates some mRNAs. The disordered region may play a role in engaging the mRNA and facilitating site selection, and so mutations in Vir1p's C-terminus should alter the distribution of m<sup>6</sup>A. Alternatively, Vir1p's C-terminal domain might facilitate interaction with a protein or proteins that help confer specificity. In the mammalian complex, there are two paralogous RNA binding proteins, RBM15/15B, that have also been implicated in site selection. Ensink et al. (2023) identified another component of the complex in yeast, Dyn2p, which is linked to the complex through Slz1p but did not find that it was orthologous to RBM15/15B or any other identified member of the complex in other organisms. There may be other components of the yeast methyltransferase complex that are yet to be identified; characterization of Vir1p's interactors might identify novel members.

Vir1p's ability to stabilize the complex might be mediated via the disordered domains acting to facilitate phase separation to sequester the other complex members away from the protein degradation machinery. In the absence of Vir1p, the proteins would not be protected and so rapidly degraded. Work has also shown that methylated mRNAs bound by reader proteins are more likely to undergo phase separation mediated by the low-complexity domains of the reader proteins (Yoon et al. 2017). Regardless of the potential role of Vir1p's disordered region, Vir1p provides several new avenues to explore mRNA methylation in yeast.

In summary, Vir1p is a conserved component of the yeast methyltransferase complex and is required for at least two steps in meiosis: an early step that is upstream of *IME1* in part through regulation of *RME1* and a later step that is at least partially upstream of *NDT80*. The high degree of conservation between the yeast methyltransferase complex and that of mammals and other

eukaryotes positions yeast as an excellent model for furthering our understanding of this important mRNA modification.

## Data availability

Source data for the RNA-seq experiments can be found using GEO accession number GSE222684.

[Supplemental material](#) available at GENETICS online.

## Acknowledgments

We would like to thank Anne Rosenwald for her helpful feedback on this manuscript. We thank Tharan Srikumar for his expert Mass Spectrometry and Emily Schmidt for technical assistance. We thank Folkert van Werven for providing the plasmid for tagging *IME1* and for sharing information before publication.

## Funding

This work was supported by NIH grants GM037739 and GM126998 to MDR.

## Conflicts of interest

The authors declare that they have no conflicts of interest.

## Literature cited

- Afgan E, Baker D, Batut B, van den Beek M, Bouvier D, Čech M, Chilton J, Clements D, Coraor N, Gruning BA, et al. The Galaxy platform for accessible, reproducible and collaborative biomedical analyses: 2018 update. *Nucleic Acids Res.* 2018;46(W1):W537–W544. doi:10.1093/nar/gky379.
- Agarwala SD, Blitzblau HG, Hochwagen A, Fink GR. RNA Methylation by the MIS complex regulates a cell fate decision in yeast. *PLoS Genet.* 2012;8(6):e1002732. doi:10.1371/journal.pgen.1002732.
- Barik A, Katuwawala A, Hanson J, Paliwal K, Zhou Y, Kurgan L. DEPICTER: intrinsic disorder and disorder function prediction server. *J Mol Biol.* 2020;432(11):3379–3387. doi:10.1016/j.jmb.2019.12.030.
- Benjamin KR, Zhang C, Shokat KM, Herskowitz I. Control of landmark events in meiosis by the CDK Cdc28 and the meiosis-specific kinase Ime2. *Genes Dev.* 2003;17(12):1524–1539. doi:10.1101/gad.1101503.
- Berchowitz LE, Gajadhar AS, van Werven FJ, De Rosa AA, Samoylova ML, Brar GA, Xu Y, Xiao C, Fitcher B, Weissman JS, et al. A developmentally regulated translational control pathway establishes the meiotic chromosome segregation pattern. *Genes Dev.* 2013;27(19):2147–2163. doi:10.1101/gad.224253.113.
- Berchowitz LE, Kabachinski G, Walker MR, Carlile TM, Gilbert WV, Schwartz TU, Amon A. Regulated formation of an amyloid-like translational repressor governs gametogenesis. *Cell.* 2015;163(2):406–418. doi:10.1016/j.cell.2015.08.060.
- Bern M, Kil YJ, Becker C. Byonic: advanced peptide and protein identification software. *Curr Protoc Bioinformatics.* 2012;40(1):13.20.1–13.20.14. doi:10.1002/0471250953.bi1320s40
- Bodi Z, Bottley A, Archer N, May ST, Fray RG. Yeast m<sup>6</sup>A methylated mRNAs are enriched on translating ribosomes during meiosis, and under rapamycin treatment. *PLoS One.* 2015;10(7):e0132090. doi:10.1371/journal.pone.0132090.

- Bodi Z, Button JD, Grierson D, Fray RG. Yeast targets for mRNA methylation. *Nucleic Acids Res.* 2010;38(16):5327–5335. doi:10.1093/nar/gkq266.
- Brush GS, Najor NA, Dombkowski AA, Cukovic D, Sawarynski KE. Yeast IME2 functions early in meiosis upstream of cell cycle-regulated SBF and MBF targets. *PLoS One.* 2012;7(2):e31575. doi:10.1371/journal.pone.0031575.
- Bujnicki JM, Feder M, Radlinska M, Blumenthal RM. Structure prediction and phylogenetic analysis of a functionally diverse family of proteins homologous to the MT-A70 subunit of the human mRNA:m(6)A methyltransferase. *J Mol Evol.* 2002;55(4):431–444. doi:10.1007/s00239-002-2339-8.
- Bushkin GG, Pincus D, Morgan JT, Richardson K, Lewis C, Chan SH, Bartel DP, Fink GR. M(6)A modification of a 3' UTR site reduces RME1 mRNA levels to promote meiosis. *Nat Commun.* 2019;10(1):3414. doi:10.1038/s41467-019-11232-7.
- Chu S, DeRisi J, Eisen M, Mulholland J, Botstein D, Brown PO, Herskowitz I. The transcriptional program of sporulation in budding yeast. *Science.* 1998;282(5389):699–705. doi:10.1126/science.282.5389.699.
- Chu S, Herskowitz I. Gametogenesis in yeast is regulated by a transcriptional cascade dependent on Ndt80. *Mol Cell.* 1998;1(5):685–696. doi:10.1016/S1097-2765(00)80068-4.
- Clancy MJ, Shambaugh ME, Timpte CS, Bokar JA. Induction of sporulation in *Saccharomyces cerevisiae* leads to the formation of N6-methyladenosine in mRNA: a potential mechanism for the activity of the IME4 gene. *Nucleic Acids Res.* 2002;30(20):4509–4518. doi:10.1093/nar/gkf573.
- Deng C, Saunders WS. RIM4 Encodes a meiotic activator required for early events of meiosis in *Saccharomyces cerevisiae*. *Mol Genet Genomics.* 2001;266(3):497–504. doi:10.1007/s004380100571.
- Dirick L, Goetsch L, Ammerer G, Byers B. Regulation of meiotic S phase by Ime2 and a Clb5,6-associated kinase in *Saccharomyces cerevisiae*. *Science.* 1998;281(5384):1854–1857. doi:10.1126/science.281.5384.1854.
- Eng JK, McCormack AL, Yates JR. An approach to correlate tandem mass spectral data of peptides with amino acid sequences in a protein database. *J Am Soc Mass Spectrom.* 1994;5(11):976–989. doi:10.1016/1044-0305(94)80016-2.
- Ensinnck I, Maman A, Albihlal W, Lassandro M, Salzano G, Sideri T, Howell S, Calvani E, Patel H, Guy Bushkin G, et al. The yeast RNA methylation complex consists of conserved yet reconfigured components with m6A-dependent and independent roles. *Cold Spring Harbor Laboratory. bioRxiv.* 2023. <https://doi.org/10.1101/2023.02.10.528004>.
- Foiani M, Nadjar-Boger E, Capone R, Sagee S, Hashimshoni T, Kassir Y. A meiosis-specific protein kinase, Ime2, is required for the correct timing of DNA replication and for spore formation in yeast meiosis. *Mol Gen Genet.* 1996;253(3):278–288. doi:10.1007/s004380050323.
- Gavin AC, Bosche M, Krause R, Grandi P, Marzioch M, Bauer A, Schultz J, Rick JM, Michon AM, Cruciat CM, et al. Functional organization of the yeast proteome by systematic analysis of protein complexes. *Nature.* 2002;415(6868):141–147. doi:10.1038/415141a.
- Guo J, Tang HW, Li J, Perrimon N, Yan D. Xio is a component of the *Drosophila* sex determination pathway and RNA N6-methyladenosine methyltransferase complex. *Proc Natl Acad Sci USA.* 2018;115(14):3674–3679. doi:10.1073/pnas.1720945115.
- Gurevich V, Kassir Y. A switch from a gradient to a threshold mode in the regulation of a transcriptional cascade promotes robust execution of meiosis in budding yeast. *PLoS One.* 2010;5(6):e11005. doi:10.1371/journal.pone.0011005.
- Guttmann-Raviv N, Boger-Nadjar E, Edri I, Kassir Y. Cdc28 and Ime2 possess redundant functions in promoting entry into premeiotic DNA replication in *Saccharomyces cerevisiae*. *Genetics.* 2001;159(4):1547–1558. doi:10.1093/genetics/159.4.1547.
- Holm L. Dali server: structural unification of protein families. *Nucleic Acids Res.* 2022;50(W1):W210–W215. doi:10.1093/nar/gkac387.
- Horiuchi K, Kawamura T, Iwanari H, Ohashi R, Naito M, Kodama T, Hamakubo T. Identification of Wilms' tumor 1-associating protein complex and its role in alternative splicing and the cell cycle. *J Biol Chem.* 2013;288(46):33292–33302. doi:10.1074/jbc.M113.500397.
- Ito T, Chiba T, Ozawa R, Yoshida M, Hattori M, Sakaki Y. A comprehensive two-hybrid analysis to explore the yeast protein interactome. *Proc Natl Acad Sci U S A.* 2001;98(8):4569–4574. doi:10.1073/pnas.061034498.
- Jin L, Zhang K, Xu Y, Sternglanz R, Neiman AM. Sequestration of mRNAs modulates the timing of translation during meiosis in budding yeast. *Mol Cell Biol.* 2015;35(20):3448–3458. doi:10.1128/MCB.00189-15.
- Kallberg M, Wang H, Wang S, Peng J, Wang Z, Lu H, Xu J. Template-based protein structure modeling using the RaptorX web server. *Nat Protoc.* 2012;7(8):1511–1522. doi:10.1038/nprot.2012.085.
- Kassir Y, Adir N, Boger-Nadjar E, Raviv NG, Rubin-Bejerano I, Sagee S, Shenhar G. Transcriptional regulation of meiosis in budding yeast. *Int Rev Cytol.* 2003;224:111–171. doi:10.1016/S0074-7696(05)24004-4.
- Kassir Y, Granot D, Simchen G. IME1, A positive regulator gene of meiosis in *S. cerevisiae*. *Cell.* 1988;52(6):853–862. doi:10.1016/0092-8674(88)90427-8.
- Knuckles P, Lence T, Haussmann IU, Jacob D, Kreim N, Carl SH, Masiello I, Hares T, Villasenor R, Hess D, et al. Zc3h13/Flacc is required for adenosine methylation by bridging the mRNA-binding factor Rbm15/Spenito to the m(6)A machinery component Wtap/Fl(2)d. *Genes Dev.* 2018;32(5-6):415–429. doi:10.1101/gad.309146.117
- Kominami K, Sakata Y, Sakai M, Yamashita I. Protein kinase activity associated with the IME2 gene product, a meiotic inducer in the yeast *Saccharomyces cerevisiae*. *Biosci Biotechnol Biochem.* 1993;57(10):1731–1735. doi:10.1271/bbb.57.1731.
- Kurihara LJ, Stewart BG, Gammie AE, Rose MD. Kar4p, a karyogamy-specific component of the yeast pheromone response pathway. *Mol Cell Biol.* 1996;16(8):3990–4002. doi:10.1128/MCB.16.8.3990.
- Lahav R, Gammie A, Tavazoie S, Rose MD. Role of transcription factor Kar4 in regulating downstream events in the *Saccharomyces cerevisiae* pheromone response pathway. *Mol Cell Biol.* 2007;27(3):818–829. doi:10.1128/MCB.00439-06.
- Lasman L, Hanna JH, Novershtern N. Role of m(6)A in embryonic stem cell differentiation and in gametogenesis. *Epigenomes.* 2020;4(1):5. doi:10.3390/epigenomes4010005.
- Lence T, Akhtar J, Bayer M, Schmid K, Spindler L, Ho CH, Kreim N, Andrade-Navarro MA, Poeck B, Helm M, et al. M(6)A modulates neuronal functions and sex determination in *Drosophila*. *Nature.* 2016;540(7632):242–247. doi:10.1038/nature20568.
- Lin S, Choe J, Du P, Triboulet R, Gregory RI. The m(6)A methyltransferase METTL3 promotes translation in human cancer cells. *Mol Cell.* 2016;62(3):335–345. doi:10.1016/j.molcel.2016.03.021.
- Liu J, Yue Y, Han D, Wang X, Fu Y, Zhang L, Jia G, Yu M, Lu Z, Deng X, et al. A METTL3-METTL14 complex mediates mammalian nuclear RNA N6-adenosine methylation. *Nat Chem Biol.* 2014;10(2):93–95. doi:10.1038/nchembio.1432.

- Mandel S, Robzyk K, Kassir Y. IME1 Gene encodes a transcription factor which is required to induce meiosis in *Saccharomyces cerevisiae*. *Dev Genet*. 1994;15(2):139–147. doi:10.1002/dvg.1020150204.
- McIsaac RS, Gibney PA, Chandran SS, Benjamin KR, Botstein D. Synthetic biology tools for programming gene expression without nutritional perturbations in *Saccharomyces cerevisiae*. *Nucleic Acids Res*. 2014;42(6):e48. doi:10.1093/nar/gkt1402.
- Mitchell AP, Driscoll SE, Smith HE. Positive control of sporulation-specific genes by the IME1 and IME2 products in *Saccharomyces cerevisiae*. *Mol Cell Biol*. 1990;10(5):2104–2110. doi: 10.1128/mcb.10.5.2104-2110.1990
- Neiman AM. Sporulation in the budding yeast *Saccharomyces cerevisiae*. *Genetics*. 2011;189(3):737–765. doi:10.1534/genetics.111.127126.
- Nesvizhskii AI, Keller A, Kolker E, Aebersold R. A statistical model for identifying proteins by tandem mass spectrometry. *Anal Chem*. 2003;75(17):4646–4658. doi:10.1021/ac0341261.
- Pak J, Segall J. Regulation of the premiddle and middle phases of expression of the NDT80 gene during sporulation of *Saccharomyces cerevisiae*. *Mol Cell Biol*. 2002;22(18):6417–6429. doi:10.1128/MCB.22.18.6417-6429.2002.
- Park ZM, Remillard M, Rose MD. Kar4 is required for the normal pattern of meiotic gene expression. *bioRxiv*. 2023. <https://doi.org/10.1101/2023.01.29.526097>.
- Park ZM, Sporer A, Kraft K, Lum K, Blackman E, Belnap E, Yellman C, Rose MD. Kar4, the yeast homolog of METTL14, is required for mRNA m6A methylation and meiosis. *bioRxiv*. 2023. <https://doi.org/10.1101/2023.01.29.526094>.
- Patil DP, Chen CK, Pickering BF, Chow A, Jackson C, Gutman M, Jaffrey SR. M(6)A RNA methylation promotes XIST-mediated transcriptional repression. *Nature*. 2016;537(7620):369–373. doi: 10.1038/nature19342.
- Perry RP, Kelley DE. Existence of methylated messenger-RNA in mouse L cells. *Cell*. 1974;1(1):37–42. doi:10.1016/0092-8674(74)90153-6.
- Poh HX, Mirza AH, Pickering BF, Jaffrey SR. Alternative splicing of METTL3 explains apparently METTL3-independent m6A modifications in mRNA. *PLoS Biol*. 2022;20(7):e3001683. doi:10.1371/journal.pbio.3001683.
- Purnapatre K, Gray M, Piccirillo S, Honigberg SM. Glucose inhibits meiotic DNA replication through SCFGrr1p-dependent destruction of Ime2p kinase. *Mol Cell Biol*. 2005;25(1):440–450. doi:10.1128/MCB.25.1.440-450.2005.
- Rappsilber J, Mann M, Ishihama Y. Protocol for micro-purification, enrichment, pre-fractionation and storage of peptides for proteomics using StageTips. *Nat Protoc*. 2007;2(8):1896–1906. doi:10.1038/nprot.2007.261.
- Ruzicka K, Zhang M, Campilho A, Bodi Z, Kashif M, Saleh M, Eeckhout D, El-Showk S, Li HY, Zhong SL, et al. Identification of factors required for m(6)A mRNA methylation in *Arabidopsis* reveals a role for the conserved E3 ubiquitin ligase HAKAI. *New Phytol*. 2017;215(1):157–172. doi:10.1111/nph.14586.
- Sawarynski KE, Kaplun A, Tzivion G, Brush GS. Distinct activities of the related protein kinases Cdk1 and Ime2. *Biochim Biophys Acta*. 2007;1773(3):450–456. doi:10.1016/j.bbamcr.2006.10.003.
- Schindler K, Winter E. Phosphorylation of Ime2 regulates meiotic progression in *Saccharomyces cerevisiae*. *J Biol Chem*. 2006;281(27):18307–18316. doi:10.1074/jbc.M602349200.
- Schwartz S, Agarwala SD, Mumbach MR, Jovanovic M, Mertins P, Shishkin A, Tabach Y, Mikkelsen TS, Satija R, Ruvkun G, et al. High-resolution mapping reveals a conserved, widespread, dynamic mRNA methylation program in yeast meiosis. *Cell*. 2013;155(6):1409–1421. doi:10.1016/j.cell.2013.10.047.
- Scutenaire J, Plassard D, Matelot M, Villa T, Zumsteg J, Libri D, Seraphin B. The *S. cerevisiae* m(6)A-reader Pho92 promotes timely meiotic recombination by controlling key methylated transcripts. *Nucleic Acids Res*. 2023;51(2):517–535. doi:10.1093/nar/gkac640.
- Sedgwick C, Rawluk M, Decesare J, Raithatha S, Wohlschlegel J, Semchuk P, Ellison M, Yates J, 3rd, Stuart D. *Saccharomyces cerevisiae* Ime2 phosphorylates Sic1 at multiple PXS/T sites but is insufficient to trigger Sic1 degradation. *Biochem J*. 2006;399(1):151–160. doi:10.1042/BJ20060363.
- Shen HF, Lan YF, Zhao YC, Shi YF, Jin J, Xie WZ. The emerging roles of N6-methyladenosine RNA methylation in human cancers. *Biomark Res*. 2020;8(1):24. doi:10.1186/s40364-020-00203-6.
- Shi HL, Wang X, Lu ZK, Zhao BXS, Ma HH, Hsu PJ, Liu C, He C. YTHDF3 Facilitates translation and decay of N-6-methyladenosine-modified RNA. *Cell Res*. 2017;27(3):315–328. doi:10.1038/cr.2017.15.
- Shin ME, Skokotas A, Winter E. The Cdk1 and Ime2 protein kinases trigger exit from meiotic prophase in *Saccharomyces cerevisiae* by inhibiting the Sum1 transcriptional repressor. *Mol Cell Biol*. 2010;30(12):2996–3003. doi:10.1128/MCB.01682-09.
- Shubassi G, Luca N, Pak J, Segall J. Activity of phosphoforms and truncated versions of Ndt80, a checkpoint-regulated sporulation-specific transcription factor of *Saccharomyces cerevisiae*. *Mol Genet Genomics*. 2003;270(4):324–336. doi:10.1007/s00438-003-0922-3.
- Smith HE, Driscoll SE, Sia RA, Yuan HE, Mitchell AP. Genetic evidence for transcriptional activation by the yeast IME1 gene product. *Genetics*. 1993;133(4):775–784. doi:10.1093/genetics/133.4.775.
- Smith HE, Mitchell AP. A transcriptional cascade governs entry into meiosis in *Saccharomyces cerevisiae*. *Mol Cell Biol*. 1989;9(5):2142–2152. doi:10.1128/mcb.9.5.2142-2152.1989.
- Smith HE, Su SS, Neigeborn L, Driscoll SE, Mitchell AP. Role of IME1 expression in regulation of meiosis in *Saccharomyces cerevisiae*. *Mol Cell Biol*. 1990;10(12):6103–6113. doi:10.1128/mcb.10.12.6103-6113.1990.
- Sopko R, Stuart DT. Purification and characterization of the DNA binding domain of *Saccharomyces cerevisiae* meiosis-specific transcription factor Ndt80. *Protein Expr Purif*. 2004;33(1):134–144. doi:10.1016/j.pep.2003.08.025.
- Soushko M, Mitchell AP. An RNA-binding protein homologue that promotes sporulation-specific gene expression in *Saccharomyces cerevisiae*. *Yeast*. 2000;16(7):631–639. doi:10.1002/(SICI)1097-0061(200005)16:7<631::AID-YEA559>3.0.CO;2-U.
- Straight AF, Marshall WF, Sedat JW, Murray AW. Mitosis in living budding yeast: anaphase A but no metaphase plate. *Science*. 1997;277(5325):574–578. doi:10.1126/science.277.5325.574.
- Teixeira MC, Monteiro PT, Guerreiro JF, Goncalves JP, Mira NP, dos Santos SC, Cabrito TR, Palma M, Costa C, Francisco AP, et al. The YEASTRACT database: an upgraded information system for the analysis of gene and genomic transcription regulation in *Saccharomyces cerevisiae*. *Nucleic Acids Res*. 2014;42(D1):D161–D166. doi:10.1093/nar/gkt1015.
- Varier RA, Sideri T, Capitanichik C, Manova Z, Calvani E, Rossi A, Edupuganti RR, Ensinnck I, Chan VWC, Patel H. N6-methyladenosine (m6A) reader Pho92 is recruited co-transcriptionally and couples translation to mRNA decay to promote meiotic fitness in yeast. *Elife*. 2022;11. doi:10.7554/eLife.e84034.
- Wang P, Doxtader KA, Nam Y. Structural basis for cooperative function of Mettl3 and Mettl14 methyltransferases. *Mol Cell*. 2016;63(2):306–317. doi:10.1016/j.molcel.2016.05.041.
- Wang X, Feng J, Xue Y, Guan Z, Zhang D, Liu Z, Gong Z, Wang Q, Huang J, Tang C, et al. Structural basis of N(6)-adenosine

- methylation by the METTL3-METTL14 complex. *Nature*. 2016; 534(7608):575–578. doi:10.1038/nature18298.
- Wei X, Huo Y, Pi J, Gao Y, Rao S, He M, Wei Q, Song P, Chen Y, Lu D, et al. METTL3 Preferentially enhances non-m(6)A translation of epigenetic factors and promotes tumorigenesis. *Nat Cell Biol*. 2022;24(8):1278–1290. doi:10.1038/s41556-022-00968-y.
- Wen J, Lv RT, Ma HH, Shen HJ, He CX, Wang JH, Jiao FF, Liu H, Yang PY, Tan L, et al. Zc3h13 regulates nuclear RNA m(6)A methylation and mouse embryonic stem cell self-renewal. *Mol Cell*. 2018; 69(6):1028–1038.e6. doi:10.1016/j.molcel.2018.02.015.
- Winter E. The Sum1/Ndt80 transcriptional switch and commitment to meiosis in *Saccharomyces cerevisiae*. *Microbiol Mol Biol Rev*. 2012;76(1):1–15. doi:10.1128/MMBR.05010-11.
- Yang Y, Hsu PJ, Chen YS, Yang YG. Dynamic transcriptomic m(6)A decoration: writers, erasers, readers and functions in RNA metabolism. *Cell Res*. 2018;28(6):616–624. doi:10.1038/s41422-018-0040-8.
- Yoon KJ, Ringeling FR, Vissers C, Jacob F, Pokrass M, Jimenez-Cyrus D, Su Y, Kim NS, Zhu Y, Zheng L, et al. Temporal control of mammalian cortical neurogenesis by m(6)A methylation. *Cell*. 2017; 171(4):877–889.e17. doi:10.1016/j.cell.2017.09.003.
- Yoshida M, Kawaguchi H, Sakata Y, Kominami K, Hirano M, Shima H, Akada R, Yamashita I. Initiation of meiosis and sporulation in *Saccharomyces cerevisiae* requires a novel protein kinase homologue. *Mol Gen Genet*. 1990;221(2):176–186. doi:10.1007/BF00261718.
- Yu H, Braun P, Yildirim MA, Lemmens I, Venkatesan K, Sahalie J, Hirozane-Kishikawa T, Gebreab F, Li N, Simonis N, et al. High-quality binary protein interaction map of the yeast interactome network. *Science*. 2008;322(5898):104–110. doi:10.1126/science.1158684.
- Yue YA, Liu J, Cui XL, Cao J, Luo GZ, Zhang ZZ, Cheng T, Gao MS, Shu X, Ma HH, et al. VIRMA Mediates preferential m(6)A mRNA methylation in 3'UTR And near stop codon and associates with alternative polyadenylation. *Cell Discov*. 2018;4(1):10. doi:10.1038/s41421-018-0019-0.
- Zaccara S, Ries RJ, Jaffrey SR. Reading, writing and erasing mRNA methylation. *Nat Rev Mol Cell Biol*. 2019;20(10):608–624. doi:10.1038/s41580-019-0168-5.

Editor: A. Mitchell